Review article

Review of the geometrical developments in GEANT4-DNA: From a biological perspective

Ruhani Khanna [a], Yvonne Reinwald [a,b], Richard P. Hugtenburg [c,d], Alejandro Bertolet [e], Ahmad Serjouei [a,*]

[a] *Department of Engineering, School of Science and Technology, Nottingham Trent University, Nottingham, UK*
[b] *Medical Technologies Innovation Facility, Nottingham Trent University, Nottingham, UK*
[c] *Swansea University Medical School, Singleton Park, Swansea, UK*
[d] *Singleton Hospital, Swansea Bay University Health Board, Swansea, UK*
[e] *Department of Radiation Oncology, Massachusetts General Hospital and Harvard Medical School, Boston, United States of America*

A R T I C L E   I N F O

A B S T R A C T

GEANT4-DNA is an expansion of the widely utilised GEANT4 Monte Carlo toolkit. This extension focuses on modelling the physical, chemical, and biological stages of ionising radiation for radiobiological applications at cellular and DNA level interactions. To date, review papers on GEANT4-DNA focus solely on evaluating a selection of the latest developments with a greater focus on mechanistic developments rather than progress in biologically specific geometries. In this work, an overview of biological analysis and biological geometries that have been developed are discussed, highlighting the latest developments and future possible development avenues for GEANT4-DNA for this application. An overview of the biological organisation levels, namely DNA, cellular, and population levels, and how GEANT4-DNA models the physical, chemical, and biological processes are also described. This review emphasises the need for persistent development of specific biological geometry accompanied by personalised DNA damage analysis parameters dependent on the biological processes considered within a specific model. It also provides an in-depth understanding of the advances at all the biological organisation levels (DNA, cellular, and population) and the use of co-operative platforms developed to model alongside GEANT4 to provide further detailed geometries and or biological damage analysis. The developments presented have been analytically discussed along with their key findings and prospects for GEANT4-DNA. Finally, a perspective on future necessary developments is portrayed since many of the advancements in the biological analysis and biological geometries discussed have not been exploited to their full potential. The development of GEANT4-DNA, using the advances discussed in this review, provides a favourable method for the evaluation of biological damage comparable to radiobiological studies.

---

* Corresponding author.
 *E-mail address:* ahmad.serjouei@ntu.ac.uk (A. Serjouei).

1. Introduction

1.1. Modelling of biological effects of ionising irradiation

Mathematical modelling has been a crucial component in radiobiology and radiation therapy since the 1920s by providing a mechanistic point of view to understanding radiation-induced biological effects [1,2]. It is essential to accurately predict the consequences following ionising radiation interaction with biological matter to enable successful therapeutic and diagnostic procedures using ionising radiation [3]. It would also provide a greater understanding to mechanisms of radiosensitivity of healthy or cancerous cells. Mathematical models influence numerous aspects of clinical practice today in radiation treatment procedures [4]. For example, the use of the Linear-Quadratic survival model, which continues to serve as the basis for evaluating the clinical equivalency of various treatment fractionation plans. Nevertheless, many models used in the clinical settings are subject to deviation when considering novel radiotherapy techniques or unique cell lines. However, many existing models show limitations when applied to newer radiotherapy techniques or novel cell lines, revealing the need for refined, context-specific approaches.

The challenge of modelling radiation-induced biological effects is compounded by the complexity of the molecular events that follow ionising radiation exposure, which occur on femtosecond timescales [5]. Given the vast number of biochemical reactions and the intricacies of cellular damage, no single model can capture all the relevant processes. This is where geometric models play a pivotal role. These models focus on the spatial distribution of radiation energy and its deposition within the target tissue, providing insights into the geometric configuration of radiation tracks and the resulting biological damage.

Monte Carlo track structure codes (MCTS) provide a superior alternative to investigate physical mechanisms of radiation damage to biological molecules affecting the DNA and cellular level by providing a general system to handle continuous interactions including interactions between tracks at nanoscales instead of sequential handling of tracks over microscopic scales. It has been widely accepted that the effects of radiation can target DNA. Track structure codes can provide details of each interaction, including single scattering models and enable an appropriate spatial resolution for small biological targets. Nevertheless, physical particle-matter interactions are not the only interactions which should be considered for modelling the biological effects of ionising radiation at the DNA level, since they are not the dominant processes at cellular level [6,7]. Physical modelling of molecular targets, descriptions of their properties and chemical interactions should also be accounted for.

While MCTS simulations provide powerful geometric insights into the physical interactions of radiation, they do not fully address the biological complexity at the cellular level. Geometric models of radiation damage must be complemented by models of the biochemical processes that follow, such as DNA repair, cell cycle progression, and cellular response to damage. Furthermore, the spatial arrangement of these processes within the cell, such as the organisation of the nucleus and the proximity of radiation tracks to critical DNA regions, requires careful geometric consideration. The integration of these physical and biological factors remains a major scientific challenge. The development of multi-scale, integrated models that combine the geometric and molecular dimensions of radiation biology is a critical area of ongoing research.
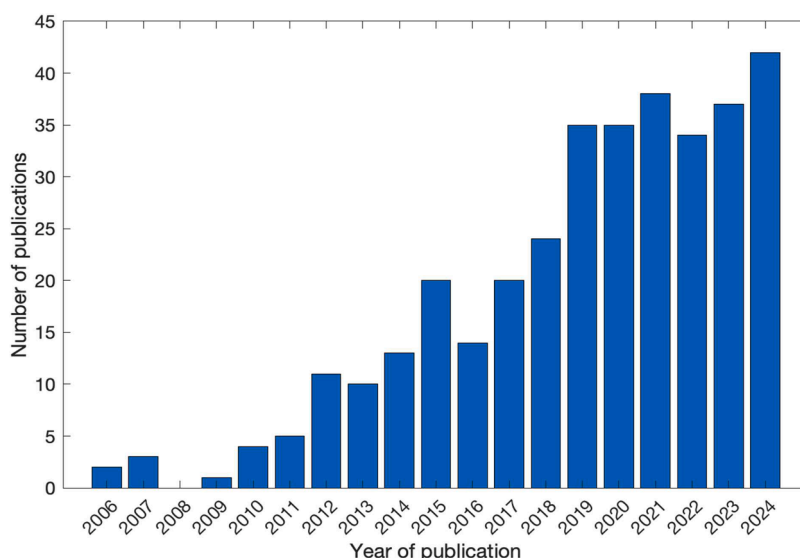
Fig. 1. The quantity of journal articles that were published between 2006 and 2024 that used 'GEANT4-DNA' as an investigative technique. To the best of our knowledge, 327 journals articles were published during this time. This research was carried out in January 2025, using the Scopus database (www.scopus.com).

1.2. GEANT4

GEANT4 is an extensively used Monte Carlo simulation toolkit for particles travelling through matter [8]. The toolkit explores energy deposited at microscopic scales by condensing many collision processes into a single step using a condensed history approach. The condensed approach of GEANT4 is insufficient to describe particle interactions at the nanoscale or DNA level since a complete description of the particle track structure is required. The importance of modelling electrons at the low electronVolt, eV, energy levels with nanoscale resolutions have been highlighted by Nikjoo and Goodhead [9]. They estimated 50 % of all ionisations to be produced by electrons with an energy of <1 keV from photon and proton beams. The low-energy limits (approximately 250 eV) of the electromagnetic physics models in GEANT4 are restricted regarding both energy range and accuracy for their implementation at the nanoscale [10,11]. The nanoscale patterns of radiation tracks and their associated energy depositions have a crucial role in the determination and formation of biological lesions [12]. There is also no water radiolysis scheme to include the production and diffusion of chemical molecules at this nanoscale.

An addition to the GEANT4 toolset, GEANT4-DNA simulates radiation interactions with biological systems at the cellular and DNA levels to predict the impacts of biological damage [13]. GEANT4-DNA is a MCTS which provides physics models reaching the very low energy domain, to around 10 eV, applicable to several materials, including liquid water, the main component of biological matter. These models can be used in addition or in combination to the models and processes provided in GEANT4. The handling of track enables all interactions on sequential, event-by-event (interaction-by-interaction) basis to be described with no condensed history approximation for applications to nanometre scale geometries. This facilitates an atomistic modelling approach suitable for the simulation of radiation interactions with cellular and DNA scale structures. Since the primary purpose of the MCTS is to simulate the detailed interactions of particles, they are accompanied by repair models which describe how biological systems recover from damage caused by radiation.

There are over 30 Monte Carlo track structure codes including PARTRAC [14], TRAX [15] and PENELOPE [16], however only few of them are publicly available and open source like GEANT4-DNA [10]. Since the introduction of the GEANT4-DNA project, several examples have been included enabling a wide range of simulations, and an increasing number of publications, as shown in Fig. 1.

In the geant4-v11.2.1 (first published on 16th February 2024) version of GEANT4, there are total of 29 examples available in the medical extended examples (/examples/extended/medical/dna), as shown in Fig. 2. Despite the development of all these extensive examples, due to their complexity, it is difficult for users to implement these examples without prior knowledge of the underpinning biology and simulation interaction models.

To date, reviews on GEANT4-DNA have focused on specific developments [19–24]. For example, detailed summary of new models regarding water radiolysis, physical, physicochemical and chemical by Bernal et al. [19] to an overview of the biological targets, new features, such as advanced chemical stage modelling, due to the complexity of "molecularDNA" example by Chatzipapas et al. [22]. However, a detailed overview of the development in biological targets has not been recently reported. This review provides summative insights into three areas. Firstly, the available modelling and DNA damage evaluation status in GEANT4-DNA. Secondly, the latest advancements in geometrical modelling at the DNA level, cellular level, cell population level and other biological structures are detailed. Thirdly, the status of co-operative platforms is presented. The increasing complexity of physics and chemistry can only be utilised to its full potential in combination with accurate and individualised biological geometry. Hence, the goal of this review is to provide a comprehensive state-of-the-art on the geometrical developments in GEANT4-DNA from a biological perspective. It also aims
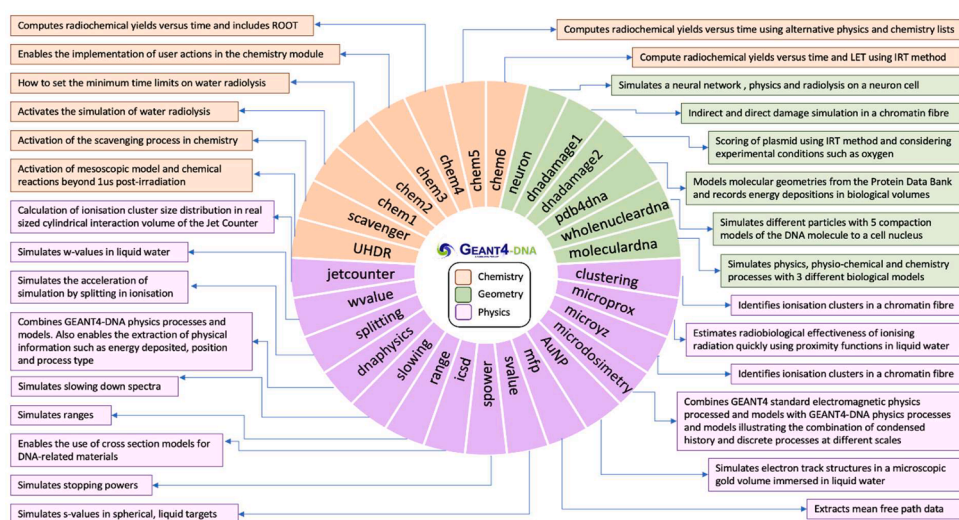

Fig. 2. Examples in the extended section of GEANT4-DNA according to the geant4-v11.2.1 version, February 2024 [17]. Orange represents chemistry-based examples, green represents geometrical examples and purple represents physics examples. Abbreviations: ROOT [18] – an object-oriented framework for large scale data analysis; LET – Linear energy transfer; IRT – Independent reaction time.

to provide guidance for further research. Subsequent research developing and merging the ability to model more accurately geometry from the DNA level to the cellular level, accompanied by more complex physical and chemical analysis will enhance our comprehension of damage of radiation on different biological structures.

2. Biological structures and damage

2.1. Critical targets for radiation damage

The DNA molecule itself is the critical target for radiation damage in the context of GEANT4-DNA simulations [25]. Simulating the direct and indirect effects of radiation on DNA requires several considerations. GEANT4-DNA can simulate the effects of radiation on DNA at various levels of abstraction, from the DNA level up to larger structures like cells. The toolkit can use a simplified representation of DNA, often modelling the molecule as a flexible chain of nucleotides, or by considering DNA double-strand breaks, which are crucial for understanding radiation-induced mutagenesis and carcinogenesis.

The toolkit includes detailed models for the interaction of ionising radiation with DNA molecules. This is typically modelled at a discrete event level to account for the stochastic nature of radiation interactions, where high-energy particles cause ionisation or excitation events in the target molecule. These events are modelled by accounting for the cross-sections of various radiation types and their interactions with the DNA. The effects of the linear energy transfer (LET) on DNA are crucial for understanding how radiation causes damage to the DNA strands. GEANT4-DNA considers spatial dose deposition, which allows for the simulation of clustered DNA damage caused by high-LET radiation which can lead to complex DNA lesions.

At a cellular level, the nucleus of a cell, where the DNA is stored, is considered a critical target in simulations. In addition to direct DNA damage, radiation can cause cellular death through apoptosis or necrosis. GEANT4-DNA incorporates simplified models for how DNA damage leads to cell death, as well as secondary effects such as cell cycle arrest and repair mechanisms.

The level of detail required for simulations in GEANT4-DNA is dependent on the requirements of the application. GEANT4-DNA offers a balance between computational feasibility and biological accuracy, which involves descriptions of parameters regarding the level of organisation modelling, such as the number of base pairs required for a DSB to be registered. To make simulations computationally feasible, molecular targets such as DNA are often simplified. For example, DNA might be modelled to consider the DNA as a material, such as liquid water, or on the atomic scale, considering each nucleotide in the DNA. This alters the computational load while still capturing the key features of radiation damage.

2.2. Organisation of the dna

GEANT4-DNA aims to model biological structures as targets. Fig. 3 illustrates the organisation of DNA in a eukaryotic cell and its sub-cellular components. While GEANT4-DNA models structures from the DNA to the whole cell, it does not currently simulate all sub-cellular components in detail. Fig. 3 highlights the relationship between a section of DNA and the formation of a protein, but components involved in this process, such as the ribosome, are not explicitly modelled within GEANT4-DNA.

A cell can be defined as the smallest structural and functional unit of an organism. DNA in a eukaryotic cell, for example, human and animal cells, is packaged as a double-stranded DNA molecule called a genome. The human genome is the complete genetic
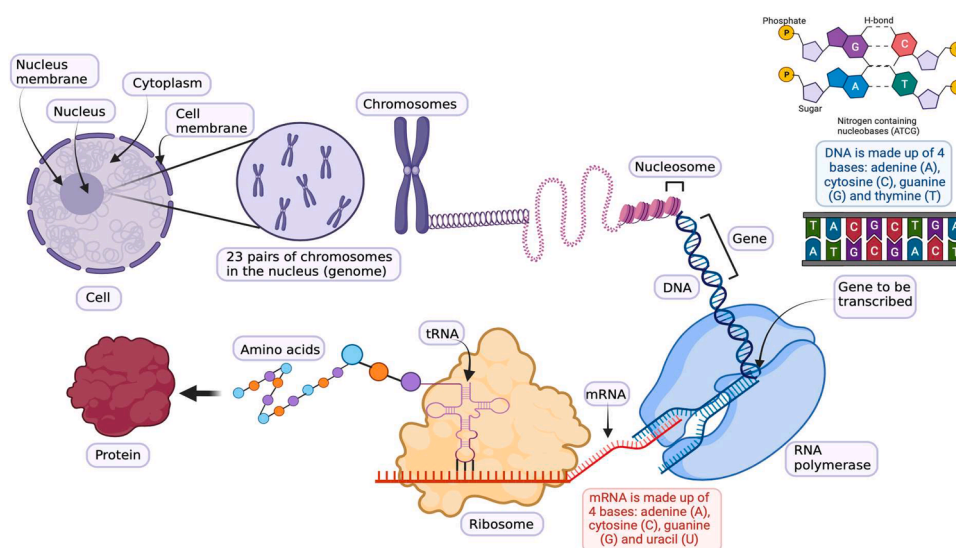
Fig. 3. Schematic of biological structures from the cellular level to the DNA level in a typical eukaryotic cell. This image was created with Bio-Render.com.

information of a human, located in the nucleus. The DNA in a eukaryotic cell is enclosed in the nucleic membrane which is surrounded by cytoplasm and held together by the cell membrane. Prokaryotic cells, for example, bacteria and virus cells, do not have their genetic material bound in a nucleus membrane which makes them different from eukaryotic cells. A single double-stranded DNA molecule in the shape of a loop or circle, known as a plasmid, makes up their whole genome. These are not essential for normal growth, however, can be exchanged with other bacteria to receive beneficial genes.

The DNA molecule itself consists of four bases: adenine, cytosine, guanine, and thymine organised in pairs. During the cell-cycle, the DNA is condensed into twenty-three pairs of chromosomes, each consisting of a linear DNA molecule. Chromosomes are non-homologous. This means that their genetic material can be different to other chromosomes. To compact the DNA into the chromosomes, the DNA is packaged into nucleosomes, DNA wound around histones. Chromosomes have two structurally and functionally distinct territories: euchromatin and heterochromatin. The euchromatin is less condensed, gene-rich (gene is defined as a section of DNA), and more easily transcribed due to its condensed state and hence the more active part of the genome. In comparison, the heterochromatin is highly condensed, gene-poor, and transcriptionally silent, hence containing similar repeating units [26].

When a gene is active a protein can be created. An RNA polymerase attaches to the gene and moves along the DNA reading the DNA sequence. As it reads the sequence a messenger RNA, mRNA, is created from free nucleotide bases in the nucleus and exits the nucleus from the nucleus pores. This process is called transcription. The mRNA binds to a ribosome, located in the cytoplasm, which reads the mRNA three bases at a time using a transfer RNA, tRNA creating an amino acid after each triplet is read. This process is called translation. Once the amino acids have been created, the chain of amino acids folds to create a protein.

2.3. Cell-specific radiation damage

To enable accurate modelling of different cell types in the context of radiation interactions, it is essential to understand the differences between cells in terms of geometry, as well as their specific biological characteristics [27]. The geometry of a cell, particularly its volume, shape, and subcellular structures, significantly influences the spatial distribution of energy deposition at the microscopic scale. The overall shape and size of a cell determine the path of incoming radiation and the degree of energy deposition within the cell. Larger cells or those with complex shapes may experience different radiation dose distributions compared to smaller, simpler cells. The presence and arrangement of organelles, particularly the nucleus, is critical since radiation-induced DNA damage is a key determinant of cellular response. The size, shape, and position of the nucleus relative to other organelles (e.g., mitochondria, endoplasmic reticulum) can affect how radiation interacts with cellular components. Variations in the cellular composition (e.g., water content, protein concentration, lipid membranes) affect how radiation energy is absorbed and dissipated. Dense, highly metabolic cells might exhibit different radiation responses compared to cells with less dense cytoplasm.

Fig. 4 shows a schematic of how different cells are created based on a single genome. Beyond the shape and cytoplasm-to-nucleus ratio, gene expression defines a specific cell and its ability to carry out its specific functions [28]. All cells have some genes called house-keeping genes which are genes expressed in all cells of a multi-cellular organism. Some genes are only expressed in certain cells. These genes code for proteins involved in essential activities for a specific cell. For example, fibroblasts have genes specifically expressed due to the mechanical loads placed on connective tissue [29]
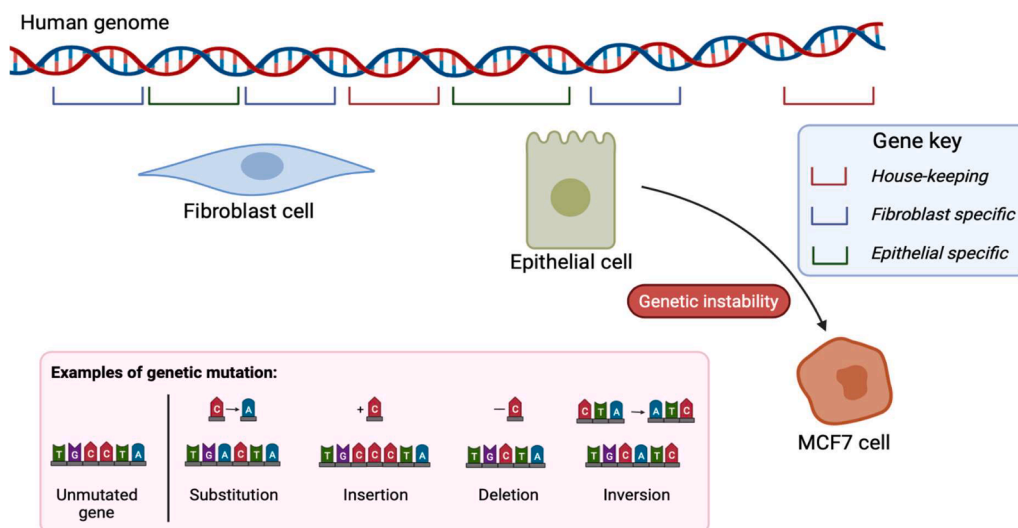
Fig. 4. Schematic of gene expression in different cell lines showing different cells can express house-keeping genes present in both cell types and express genes specific to the cell type. The schematic also shows examples of genetic mutation which leads to genetic instability and the creation of a cancer cell, such as an MCF7 cell from the genetic instability developed from an epithelial cell. There are several methods for genetic mutations including substitution, insertion, deletion, and inversion. These genetic mutations are changes within the DNA sequence using the four bases in the DNA: adenine, cytosine, guanine, and thymine. This image was created with BioRender.com.

When DNA mutations occur, they lead to changes in the base pair structure, the formation of the nucleus, and chromatin compaction. These alterations also affect cell structure, function, and the proteins produced [30]. This alters the cellular behaviour leading to genetic instability. A high frequency of mutations within a cellular lineage's genome that give rise to cancer is known as genetic instability. There are many methods for genomic instability based on the rearrangement of the DNA sequence containing the four bases adenine, cytosine, guanine, and thymine. Examples of genetic mutations found in cancer cells include missense, nonsense, and frameshift mutations and chromosome rearrangements.

The primary objective of any radiation treatment is to increase the radiation dose to aberrant cancer cells while restricting exposure to normal cells that are nearby or in the radiation's trajectory. While both healthy and cancerous cells are damaged by radiation, normal cells can predominantly repair themselves more rapidly while preserving their regular functioning state in comparison to cancer cells. Cancer cells typically are less effective than healthy cells in repairing radiation-induced damage, which leads to differential cancer cell killing [31]. The differences are heavily based on the type and structure of the cell.

The nucleus to cytoplasm volume ratio in healthy cells is generally lower than many cancerous cells [32]. This would in turn affect the spatial distribution of ionisations occurring outside the nucleus and could greatly influence the damage observed and the biochemical pathways triggered due to the spatial variations in chemical composition and densities of sub-cellular structures. Numerous diseases are largely influenced by alterations in a cell's shape and structure.

Mutations that lead to cancer can prompt cells to become amorphous and malleable by causing them to lose the adhesions that hold them to neighbouring cells. This gives the cancer cells freedom to spread to and proliferate in other bodily regions. The overall shape of the cell is fundamental not only in cancer detection, but also for curative purposes. Despite the progression of understanding behind the basic principles of ionising radiation on individual biological systems, less is understood about the key differences between the behaviour of healthy and cancerous cells from ionising irradiation.

However, there remains a gap in modelling the differences between various cell types, especially in comparing cancerous and healthy cells. While there has been progress in simulating radiation-induced damage, these models often rely on simplified or homogeneous cell representations, with a limited consideration of cell geometry and composition. For example, many current simulations treat the cell as a single, uniform entity, typically using water as a substitution for cellular composition, which oversimplifies the complex biological environment. Water is frequently assumed to represent the medium within cells due to its high prevalence and relatively simple interactions with radiation, but it is important to recognise the limitations of this assumption. Water's role is often overemphasised, and its use as a model for the cell's biochemical and structural complexity may not accurately reflect the intricate behaviour of various cellular components, such as proteins, lipids, and nucleic acids.

The lack of detailed, accurate representations of both cancerous and healthy cells, considering their unique geometric and chemical properties, limits our ability to fully understand radiation-induced damage at the micro and nanoscale. Future simulations that incorporate more precise modelling of cell geometry, composition, and microstructural details could enhance our understanding of biological damage, offering valuable insights into experimental findings. However, the current limitations of computational models,
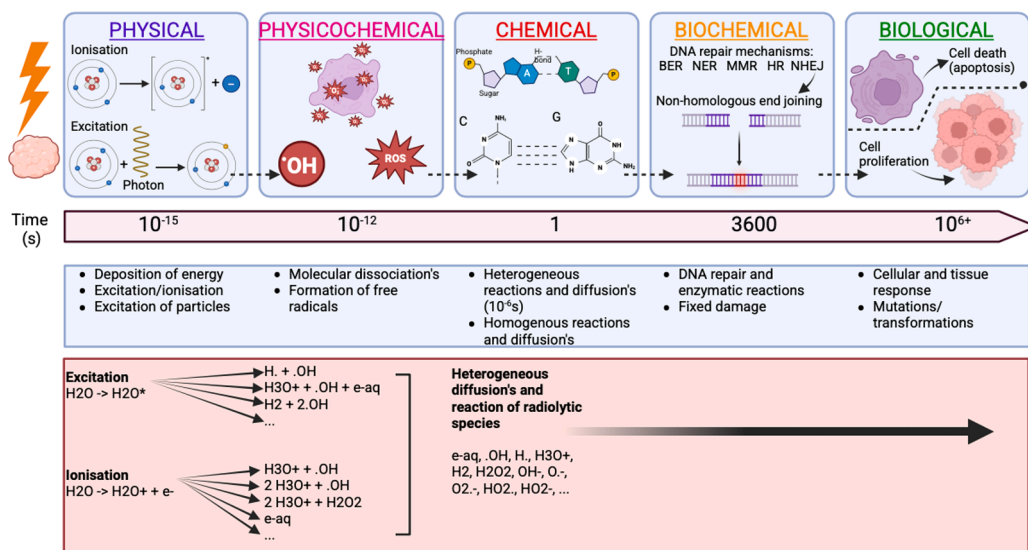
Fig. 5. The phases of damage occurring over time from ionising irradiation on biological matter. (1) Physical - occurring from ionisation and excitations from interactions of charged particles with matter. (2) Physicochemical – creation of radiolytic products such as free radicals. (3) Chemical – heterogeneous and homogeneous reactions and diffusions within the cell. (4) Biochemical - DNA repair mechanisms, examples include BER (Base Excision Repair), NER (Nucleotide Excision Repair), MMR (Mismatch Repair), HR (Homologous Recombination) and NHEJ (Non-homologous End Joining). (5) Biological – cellular and tissue response and long-term effects. The phases of damage according to the water radiolysis as implemented in GEANT4-DNA. The image is adapted from Chappuis et al. [23]; the full list of dissociation channels is available in Ref. [33]. This image was created with BioRender.com.

particularly in their oversimplification of cellular environments, should be carefully considered when interpreting simulation results. Future simulations using accurate cell composition both geometrically and chemically and of both cancerous and healthy cells would help to understand biological damage occurring at the micro and nanoscale, extending our understanding of experimental activity.

2.4. Damage from ionising irradiation implemented in GEANT4-DNA

Biological damage from ionising radiation is a complex sequence of events including damage to DNA, lipids, proteins, and metabolites amongst others. Biological effects also depend on several factors based on their nature and timing after exposure. Damage from ionising radiation occurs in five phases: physical, physicochemical, chemical, biochemical and biological, as shown in Fig. 5 (adapted from Chappuis et al. [23]; the full list of dissociation channels is available in the work of Shin et al. [33]).

GEANT4-DNA uses macroscopic geometry to track particle interactions and energy deposition at the cell and tissue level but then shifts to molecular-scale geometry to model the biochemical consequences of these interactions (e.g., DNA damage, radical formation). The modelling framework allows for a multiscale approach, transitioning from the physics of particle interactions (at the cellular or tissue level) to the chemical effects of energy deposition at the molecular and atomic levels, with detailed geometric representations of individual molecules like DNA. The geometric representation of the DNA molecule, or other biomolecules, is used to model how close these radicals are to key sites within the molecule, like sugar-phosphate backbones or bases in the case of DNA, and how they might cause damage, such as strand breaks or base modifications.

The following sub-sections will describe both the damage occurring biologically from ionising radiation and how GEANT4-DNA implements damage analysis for these different phases of damage: physical, physicochemical, chemical, biochemical, and biological.

2.4.1. Physical processes

The physical damage consists of the deposition of energy from charged particle interactions with matter, such as ionisation and excitation. These processes involve the generation of electrons typically lasting for 10^{-15} s. GEANT4-DNA describes the physical interactions as processes using different models. These models use a sequential event-by-event (interaction-by-interaction) process of physical interactions of radiation with biological medium. The models, which may be theoretical or semi-empirical, are responsible for the computation of the physical interaction and full depiction of the final system, including the production of secondary particles, energy loss and emission angles [19]. The theoretical models are derived from fundamental principles of physics, such as the electron scattering models or the continuous energy loss models, where the energy loss of charged particles is based on fundamental interactions such as the Bethe-Bloch formula [34]. The semi-empirical models incorporate experimental data to refine their predictions for example, for track structure models which may use parameters fitted to experimental data to describe the distribution of energy deposition along a particle's track. In GEANT4, all required particles, processes and models are defined by a "physics constructor" [35]. GEANT4-DNA currently has nine physics constructors: G4EmDNAPhysics and G4EmDNAPhysics, options 1 to 8. There are three key physics constructors: option 2, 4 and 6. The G4EmDNAPhysics_option2 was the first set of models applied, simulating electron interactions up to 1 MeV as well as all other particle interactions, however, it contained deficiencies of inelastic modelling. These deficiencies include limited cross-sectional data, insufficient energy transfer calculations or oversimplified modelling. It also enabled more accurate simulations of stopping powers, dose point kernels and W-values in liquid water. G4EmDNAPhysics_option4 is most used and provided an alternative model for inelastic models including an updated cross-section for excitation and ionisation. This option is the recommended and mostly used option for interactions at the DNA levels as it contains electron elastic and inelastic models up to 10 keV and is being extended up to 10 MeV. G4EmDNAPhysics_option6 allowed the implementation of the cross-section models describing interactions electrons, elastic and inelastic models, in liquid water up to 255 keV obtained from the CPA100 code, another Monte Carlo track structure code, enabling the DNA material interactions [36]. Further information on these constructors, processes and models can be found in literature [10]. The selection of the physics constructor is often based on the type of the simulation required by the users' application and the interaction of the particle of interest under investigation. The selection of the physics constructor is often based on the application requirements and the interaction of the particle of interest under investigation. The choice of physics constructor has been shown to be most important when using electrons in comparison to protons or hydrogen [35].

2.4.2. Physicochemical processes

The secondary electrons, in the physicochemical phase, begin to create radiolytic products such as free radicals, between 10^{-15} and 10^{-12} s. The main products of radiation in water are hydrated electrons, e_{aq}^-, hydroxyl radicals $HO^\bullet$, hydrogen radicals $H^\bullet$, radiolytic hydrogen H_2, hydrogen peroxide H_2O_2 and hydroperoxyl radical $HO_2^\bullet$.

2.4.3. Chemical processes

GEANT4-DNA can also simulate the water radiolysis in an irradiated medium up to 1 μs after irradiation for different biological targets at the micro and nanometre scale [35]. This means interactions from the homogeneous chemical diffusion and their onward paths. For accurate simulations, water radiolysis must be carefully implemented into the definition of damage phases within GEANT4-DNA. The reactions and scheme of damages implemented over the three phases is shown by Fig. 5.

GEANT4-DNA utilises a dissociation channel according to the mode of electronic alterations that the water molecules undertake along with the appropriate branching ratios that the user has preselected. A water molecule is decomposed within the physical stage where water molecules dissociate. This occurs if the water molecules are either ionised or undergo electron attachment. The physicochemical stage starts with the creation and distribution of radiation-induced spurs along the axis of the tracks [37], this is the water radiolysis production stage. The chemical stage occurs breaking up spur, diffusing the molecules which are later described

homogenously after 1 µs from the initial irradiation. The location of the dissociation products, immediately following dissociation, in time and space presents a challenge in simulating the chemical phase of damage from ionising irradiation. Currently, empirical root-mean-squared distance and momentum conservation are used to calculate these initial positions, with the chemical species being described by the Brownian motion. Due to the step-by-step definition of the diffusion of particles, all species are diffused within a time step and placed in a new position. A reaction occurs when the distance between two Brownian particles is less than a reaction radius. Hence the time step is computed to verify whether a reaction has occurred in GEANT4-DNA, presented by a constructor called G4EmDNAChemistry with options 1, 2 and 3. The original G4EmDNAChemisty was implemented with parameter values from PAR-TRAC [38]. Option 1 was implemented a set of chemistry parameters from Shin et al. [33], option 2 included chemistry parameters for reactions with DNA components and option 3 implements the independent reaction time (IRT) approach from Ramos-Mendez et al. [39]. The successive chemical reactions occur, starting the DNA damage formation from 10^{-12} to 1 s. The free radicals react with the biomolecules such as the DNA, lipids, and proteins in addition to the cell redox status changing between 1 and 3600 s. Currently, GEANT4-DNA can simulate the initial production of free radicals and their interactions with biomolecules; it cannot directly simulate the dynamic changes in redox status of the cell. Dynamic changes in a cell's redox status refer to fluctuations in oxidant and antioxidant levels in response to internal and external stimuli, such as metabolic activity, environmental stressors, and cellular damage. These fluctuations are tightly regulated, as they play a crucial role in key biological processes, including cell signalling, gene expression, apoptosis, and DNA repair. While maintaining a balanced redox state is essential for cellular function and survival, GEANT4-DNA does not currently model these dynamic changes directly. The modelling of cell redox status changes would require additional modelling frameworks or integration with biochemical models.

GEANT4-DNA can model the diffusion of species in addition to the reaction mechanism by either using the step-by-step (SBS) method, independent reaction time (IRT) method, or the IRT sync method [40]. The SBS method computes the trajectory of species on a step-by-step diffusion basis, where two species react when their separation distance is below a defined threshold. This can become computationally exhaustive. Compared to the SBS technique, the IRT method offers a higher computational efficiency by computing random timings of reaction from the initial position of the species. Then the reactions occur one by one starting with the shortest reaction times. The higher computational efficiency also comes with loss of information on the position of the radiolytic species over time. The IRT sync method is an IRT approach with a time step limitation, where IRT sync stores all the molecular positions at each time step like the SBS method.

Radiation-based Monte Carlo simulations on a simplified pure liquid model are not appropriate for generating radioactive species in environments that are relevant to biology. This limitation arises from the model's inability to account for the heterogeneity of biological systems (e.g., assuming pure water instead of biological materials and neglecting the complexity of cellular structures such as organelles), specific molecular interactions (e.g., the spatial organization of DNA within a cell), and chemical reactions beyond ionisation and excitation (e.g., oxidative damage mechanisms). A more accurate simulation requires detailed models that incorporate biomolecular structures, spatial organisation, and dynamic biological processes, such as DNA damage, repair pathways, and radical reactions. As a result, in simulation the addition of the chemical impact of uniformly distributed molecules, also referred to as scavengers, are required.

The application of a comprehensive structure for scavenger utilisation is being studied by GEANT4-DNA. The inclusion of competing chemical reactions, where scavengers interact with radiation-induced species, significantly disturbs the radiolysis mechanism. For example, in the presence of scavengers, hydroxyl radicals may react with these molecules before they can interact with DNA, potentially reducing DNA damage. Chappuis et al. [23] investigated the SBS and IRT models, validating their implementation in Geant4-DNA through comparisons with other Monte Carlo track-structure codes. Their findings highlighted the role of macromolecules, such as lipids and plasmids, as scavengers that influence the distribution, reactivity, and lifetime of reactive species within the cell. These mechanisms, in turn, impact biological outcomes, including DNA damage and repair processes. Furthermore, their study underscored the importance of extending simulations to incorporate the homogeneous chemical stage, enabling a more accurate representation of cellular scavenging effects at the mesoscopic level.

2.4.4. Biochemical processes

The biochemical stage involves damage to the cellular components which triggers a cascade of biochemical events. This refers to alterations at the molecular and chemical level within the cell that disrupt normal biological functions. This type of damage can occur to various cellular components including the DNA, proteins, lipids and other biomolecules. The type of biochemical damage includes DNA damage, protein damage, lipid peroxidation, altered metabolites and mitochondrial damage. Once the damage occurs, the cell enters a phase where DNA repair mechanisms are activated, and a variety of enzymatic reactions take place to restore cellular integrity. Concurrently, alterations in key cellular pathways may occur, influencing processes like cell cycle regulation, apoptosis, and survival signalling. Based on the extent of the damage and the effectiveness of repair, the cell may then proceed to one of several outcomes. The cell can either proliferate, or survive but no longer proliferate, or undergo cell death through apoptosis, necrosis, or autophagy.

2.4.5. Biological processes

The biological phase of radiation damage can span a wide range of timescales, from minutes to years [41]. The extent of the damage depends on several factors, including the efficiency of repair mechanisms, the type of radiation, and the quantity and complexity of the induced damage. Radiation is typically classified into two categories based on its LET: high LET (e.g., alpha particles, protons, and neutrons) and low LET (e.g., electrons, gamma rays, and X-rays) [42]. LET refers to the average amount of energy a particle loses per unit of distance travelled through tissue. Low LET radiation tends to produce a low concentration of ionisation events along its track, leading to isolated damage sites. In contrast, high LET radiation causes a high concentration of ionisation events, resulting in more

complex damage, including clustered lesions. Approximately 70 % of the energy deposited by low LET radiation results in isolated lesions, while around 90 % of the energy deposited by high LET radiation leads to clustered damage sites [43].

DNA damage can be produced through either direct or indirect action. Direct damage occurs when radiation damages the DNA by the deposition of energy directly into the DNA molecule. GEANT4-DNA classifies a direct damage when sufficient energy is deposited in proximity of the sugar phosphate group. The proximity can be defined by a radius or a hydration shell, where the energy threshold can be defined as a linear probability from 5 eV to 37.5 eV [44–47] or as a fixed threshold limit of 17.5 eV [14,48–50]. When secondary electrons and primary radiation interact in the molecular environment around DNA, chemical species are produced that could lead to indirect damages. In GEANT4-DNA strand breaks occur when free radicals interact with the DNA. The activation probability defines if these reactions classify as a strand break; this is defined by diffusion coefficients and reaction rates. Both indirect and direct damage can cause single strand breaks (SSBs), double strand breaks (DSBs), base modifications, and DNA helix distortions. However indirect damages mostly cause SSBs, and DNA base modifications which contribute to an increased complexity of a lesion [51]. DSBs are considered most lethal since they can cause genomic instability and cell death. DSBs are defined by a break in the phosphor-based backbone of both strands of the DNA generally separated by a user defined number of base pairs (bp) [43]. The secondary electrons generated in ionising radiation interactions are primarily in charge of the energy deposition on the DNA. For a nanometric description of the track structure to be obtained, an exhaustive description of their transport is thus required. GEANT4-DNA uses the information from the simulation such as energy deposition, in addition to the chemical reaction outcomes to infer biological damage using semi-empirical biological repair prediction models, such as cell survival. In GEANT4-DNA, three repair models have been applied: the Local Effect Model IV (LEM IV) which uses non-re-joined DSB as its endpoint [52], the Two Lesion Kinetic Model (TLK) which uses the survival fraction as its endpoint [53], and Belov model which uses DSB repair as its endpoint [54]. Their implementation enables the quantification of protein and enzyme kinetics, DNA re-joining and cell survival.

The examples in GEANT4-DNA discussed henceforth in the review, are examples which demonstrated geometrical and biological damage simulation capabilities, going beyond physics and chemistry. Incorporating biological repair mechanisms into GEANT4-DNA is essential for extending damage estimation beyond microseconds, the longest duration that GEANT4-DNA's simulation of water radiolysis can achieve. The following sub-sections discuss the biological damage analysis in each of these examples. Detailed descriptions of the various GEANT4-DNA examples and their agreement with other track structure codes can be found in literature [19, 35], however the use of biological damage quantification and repair models is summarised here.

2.4.5.1. Density-based clustering algorithm approach. The "wholeNuclearDNA" example [55] was created to determine the relative quantification of the number of direct complex damages resulting from proton irradiations dependent on the cell type and the density of DNA within the nuclei of the cells. This example outputs information about the type of particle per step, process per step, location of damage based on which strand of the DNA was hit, and details of the energy depositions and step length of the tracks. The information about the tracks is analysed by the density-based clustering algorithm, DBSCAN [56]. The DBSCAN works on the assumption that clusters are dense regions in space separated by regions of lower density, as shown in Fig. 6. Subsequently, it groups the denser group data points into a single cluster. Such clustering algorithms are prevailing tools to recognise and define groups and the links between them. In comparison to other algorithms, the DSBCAN is computationally proficient and requires only two input parameters: the radius of the neighbourhood area and the minimum number of points needed to form a cluster [57,58]. The location of energy transfer events in the DNA-sensitive volumes in relation to potential double helix damage is defined by the "wholeNuclearDNA" example. All the registered inelastic interactions would then be processed by the clustering algorithm. This selection would solely consider direct damages. Hence, the "wholeNuclearDNA" example enabled the evaluation of direct damages in geometrically cell-based models. The advanced geometry of a fibroblast cell highlighted the need for accurate cell geometry for accurate biological damage analysis.

The "clustering" example extends the use of the DBSCAN algorithm and investigates the pattern of energy deposition on a simplified cell geometry. The geometry used in this example is a simple target box of 1 μm × 1 μm × 0.5 μm; so, the track simulations could be carried out in micron scale volumes representing DNA containments. There are necessary parameters defined in the "clustering"
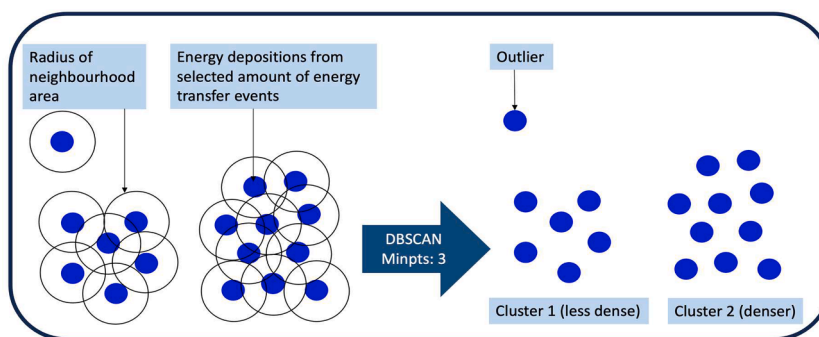
Fig. 6. A representation of the DBSCAN algorithm where the radius of the neighbourhood area is defined. The minimum points to define a cluster is given as 3 as an example. The DBSCAN then defines a cluster depending on the densities and difference in densities. This image was adapted from Khater et al. [59]. Abbreviations: MinPts - minimum points per cluster.
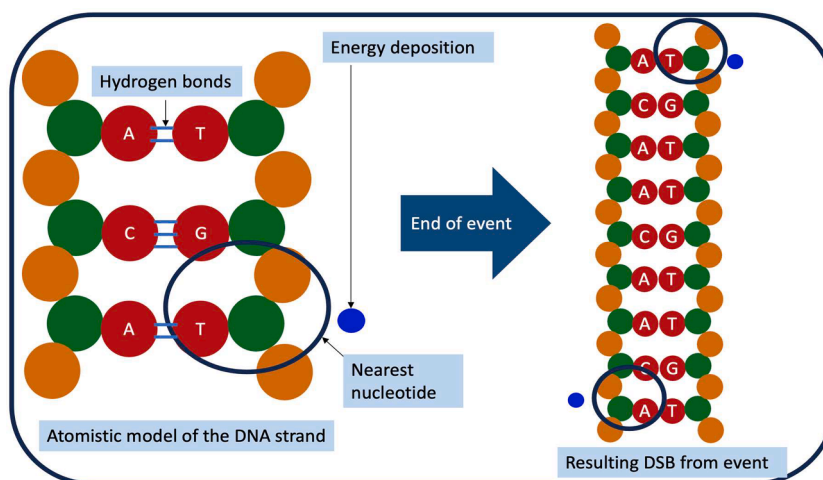
Fig. 7. A schematic of the algorithm used in the "PDB4DNA" example, where an energy deposition is assigned to nucleotides. Then the assignment is evaluated at the end of each event to determine the biological damage. In this case, since there are two energy depositions within 10 base pairs and on opposite strands, this is classified as a DSB.

example, which can be adjusted by the user: neighbourhood radius of a point (eps), minimum points per cluster (MinPts), the probability that a point falls in a sensitive area from which it can directly or indirectly reach the DNA (SPointsProb) and the energy bounds (EMinDamage & EMaxDamage). The default selection of the values for these parameters are based on biological parameters; for example, the eps is usually set to 3.2 nm representing the distance within two SSBs to be considered as a DSB since this is the size of ten base pairs. Similar to Fig. 6, once the clusters are formed, the code scans all clusters once and merge them if their barycenters are separated by less than the maximum distance selected by the user. Alongside the latest GEANT4-DNA physics models, SSBs, complex SSBs, DSBs and cluster sizes can be evaluated.

2.4.5.2. The computematchedepdna algorithm. The "PDB4DNA" example focuses on the interaction descriptions on a DNA level to estimate the number of direct SSBs and DSBs [10]. The example uses a dinucleosome geometry extracted from the "1ZZB" file, obtained from the Protein Data Bank, PDB [60]. The PDBlib::ComputeMatchEdepDNA algorithm used in this example is used to find the closest atom to each energy deposition. Fig. 7 pictorially presents a simplification of this example's energy deposition. This specific algorithm is optimised for the DNA molecule and no other stereochemical conformation. The algorithm aims to assign the energy deposition to a sphere bound with a nucleotide, where the centre of a bound sphere is understood as the geometrical barycenter of a nucleotide, hence only nucleic structures can be implemented in this example. The radius here is defined as the maximum distance between the barycentre and atom coordinates creating the nucleotide, including the maximum Van der Waals radius, 1.8 Angstrom for the element phosphor.

Once an energy deposition is assigned to a bound sphere, the Van der Waals radii are checked to locate the atom of the nucleotide nearest the energy deposition. The nearest two nucleotides are included in the algorithm since the nucleotide bound spheres overlap. Upon determining a pair, the algorithm returns the energy deposition, the DNA strand, the nucleotide identifier, and the group identifier (base, phosphate, or sugar group). The assessment of biological damage is the next phase of analysis in this example. SSBs are determined using a minimum energy deposition of 8.22 eV, corresponding to the first excitation energy level of liquid water in GEANT4-DNA models in the sugar-phosphate backbone which can be user adjusted. DSBs are defined when a maximum distance of 10 bp are separating two SSBs on opposite DNA strands [61].

At the beginning of the simulation, an empty associative map is created for each DNA strand. The nucleotide identification and energy deposition are recorded if either strand is not empty after tracking a primary particle and all its secondaries. The maps are updated each time the closest atom is successfully identified. These maps are then read at the end of each event to compute the number of SSBs and DSBs, using the approach where a certain distance must be defined between the strand breaks to classify as a DSB.

2.4.5.3. Direct and indirect damage classification. The "dnadamage1" example focuses on the inclusion of the indirect effects of DNA damage, a shortcoming in all the examples explained so far, by classifying damages based on the source of damage. Direct damage is defined by the radius and the energy bounds for an event to create a strand break [62]. This radius is defined as the distance from the DNA molecules at which energy depositions will be considered to interact with the DNA molecules. These DNA molecules are defined as six molecules representing sugar, phosphate, and 4 bases encompassed in a hydration shell. The indirect damage is characterised based on the reaction that can produce damage and its probability. The chemistry lists enable the differentiation of the energy required to break the bonds between the different base pairs. This emphasises the need for DNA specific geometry.

The characterisation of breaks and their complexity is based on a scheme proposed by Nikjoo et al. [63] initiated in the "dnadamage1" example. Tables 1 and 2 describe the available characterisation of breaks and their complexity, after further development
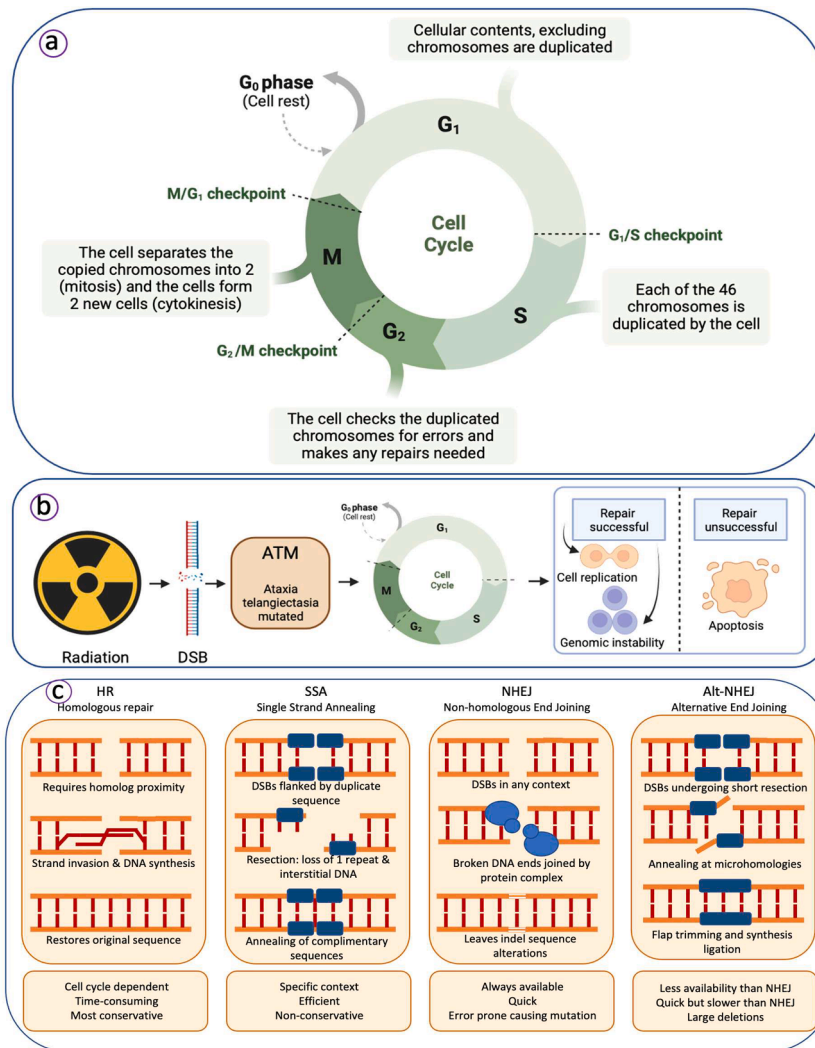
Fig. 8. (a) An explanation of the cell cycle with the cell cycle checkpoints highlighted as the possible points of repair. (b) The timeline of the repair including the irradiation, creation of a DSB and the repair. (c) A schematic of homologous recombination (HR), nonhomologous end joining (NHEJ), single strand annealing (SSA) and alternative end joining (alt-NHEJ), also known as microhomology-medicates end joining (MMEJ). This image was created with BioRender.com.
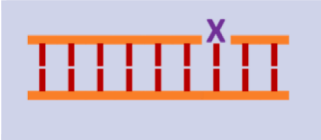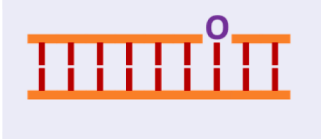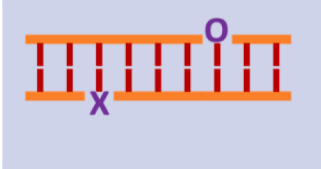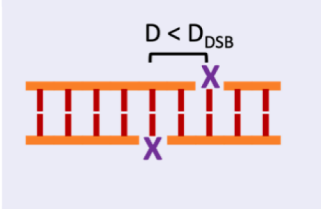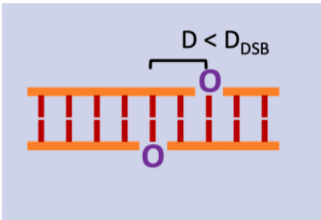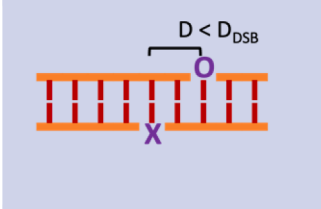
from the initial implementation in the "dnadamage1" example to the later examples such as in "molecularDNA". These tables provide details about the source of damage and the complexity of SSB and DSB. These specific details are valuable to investigate different processes of DNA damage induction and hence enable the user to investigate the specific damage repair mechanisms. Two key parameters are defined in the tables, and hence define the damages: (1) D_{DSB} which is the maximum separation between two break events on opposite DNA strands to be considered independently as a DSB, typically 10 bp; (2) Ds which is the length of undamaged base pairs required for two damaged segments to be considered independently, typically 100 bp.

2.4.5.4. DNA damage repair models. To increase the complexity of the defined biological damage in GEANT4-DNA, the "molecularDNA" example, includes DNA damage repair models for irradiated cells based on the mathematical approach outlined by Belov et al. [54] and further examined by Sakata et al. [64]. DNA repair is the procedure in which a cell maintains the integrity of its genetic code. Repairs for simple lesions, a damage or change within the cell caused by trauma or disease, can be independently carried out. The repair of more complex lesions, with multiple DNA processing steps, is regulated by the DNA damage response (DDR) [65,66]. There are different DNA repair pathways for the repair of different damages. Homologous recombination (HR), nonhomologous end joining (NHEJ), single-strand annealing (SSA) and alternative end joining (alt-NHEJ) are the main pathways for DSB repairing [67].

Fig. 8 shows the biological processes involved in the repair process. The enzyme Ataxia Telangiectasia Mutated, ATM kinases, are activated in response to DNA damage, by activating enzymes to fix the broken strand, initiating a cellular response (Fig. 8b). At various checkpoints, the cell cycle is stopped to try and repair the damage (Fig. 8a). A cell-cycle has two major phases: interphase (G_1, S, and G_2

Table 1

A description of the damage classifications in GEANT4-DNA. These classifications are analysed based on the source of the damage. Denotations represent the source of the damage, namely direct, d, indirect, i, mixed, m, and hybrid, hyb. This table was inspired by Nikjoo et al. [63].

Damage	Type of DNA damage	Definition (source of damage)	Representation of DNA damages
SSB_d	Simple SSB	The SSB includes only direct (X) damages	
SSB_i	Simple SSB	The SSB includes only indirect (O) damages	
SSB_m	Complex SSB	The 2xSSB*, 2SSBs** or SSB+ include both direct and indirect breaks	
DSB_d	Simple DSB	The DSB includes only direct damages D: Distance between damages D_{DSB}: Maximum distance between damages to give a DSB	
DSB_i	Simple DSB	The DSB includes only indirect damages	
DSB_m	Complex DSB	The DSB+ or DSB++ include both direct and indirect breaks	
DSB_{hyb}	Complex DSB	The DSB contains both a direct and indirect damage	

* 2xSSB refers to two SSBs as independent damages; refer to Table 2 for further explanation.

** 2SSB refers to the SSBs on opposite strands too far apart to be considered as a DSB; refer to Table 2 for further explanation.

Table 2

A pictorial representation and description of the damage classifications in GEANT4-DNA. These classifications are analysed based on the complexity of the damage. Denotations represent the source of the damage, namely direct, d, indirect, i, mixed, m, and hybrid, hyb. This table was inspired by Nikjoo et al. [63].

Damage	Type of DNA damage	Definition (damage complexity)	Representation of DNA damages
SSB	Simple SSB	A single damage of either direct or indirect nature	
2 x SSB*	Multiple isolated SSBs	Two SSBs as independent damages D_S: Minimum length of undamaged base pairs required for two damaged segments to be considered independently (100 bp)	
SSB+	Complex SSB	Two SSBs as complex damages since they are within the same damaged segment under analysis	
2SSB**	Simple SSB cluster	The SSBs on opposite strands too far apart to be considered as a DSB but less than D_s	
DSB	Simple DSB	Damages are less than D_{DSB} D_{DSB}: Maximum distance between damages to give a DSB	
DSB+	Complex DSB	A DSB and at least one additional break within D_S	
DSB++	Complex DSB	At least 2 DSBs within D_S	

* 2xSSB refers to two SSBs as independent damages.
** 2SSB refers to the SSBs on opposite strands too far apart to be considered as a DSB.

phases), where the cell grows and makes a copy of its DNA; mitotic (M) phase, where the cell separates its DNA to form two new cells. If the repair is successful, either cell replication or genetic instability will occur. If the repair is unsuccessful cell apoptosis will occur. Fig. 8c briefly presents the DSB repair pathways of homologous recombination (HR), nonhomologous end joining (NHEJ), single strand annealing (SSA) and alternative end joining (alt-NHEJ), also known as microhomology-medicates end joining (MMEJ).

Considering these four DSB repair pathways, the model in GEANT4-DNA calculates the accumulated repair protein yield by

considering the number of repairable and non-repairable DSBs (DSB+ and DSB++) per unit of dose per cell. The model implemented in GEANT4-DNA applies the mass-action kinetics approach. The mass-action kinetics approach uses the law of mass action which sets the foundation of the kinetics of chemical reactions. The law states that the rate of reaction is proportional to the chemical activities of the reactants involved where the chemical activity depends on concentrations of the reactants. The rate constants used in the model are evaluated using y-H2AX foci experimental data on the kinetics of different stages of DSB repair. y-H2AX is involved in the cellular response after a DSB and hence can be used as a biomarker of radiation exposure monitored over time.

In addition to the y-H2AX analysis, the "molecularDNA" example also enables survival fraction evaluation, a common radiobiological assay, based on the TLK model proposed by Stewart et al. [53], shown in Fig. 9. The survival fraction analysis allows the cell viability to be determined based on the proportion of live, healthy cells within a population. The TLK model uses the subdivisions of each kind and complexity of DSBs, each with their own fast or slow DNA repair characteristics to calculate the survival fraction of a cell population 14 days after an irradiation based on the experimental procedure by Suzuki et al. [68], where a colony was defined with >50 cells kept in 5 % CO_2 incubation at 37 °C after 14 days. Additionally, the DNA fragments associated with the DSB can interact with each other in pairs and form lethal or non-lethal chromosomal aberrations.

The "dsbandrepair" example bases its geometry in the DNAFabric tool, where voxels of "straight", "up", "down", "right" and "left" are used to create DNA conformations for both the heterochromatin and euchromatin regions. The addition of the heterochromatin and euchromatin was a key difference from the "molecularDNA" example. The geometry in the "molecularDNA" example is modelled using FractalDNA, a package in python [46]. Three geometries are presented in this example namely, human fibroblast, human endothelial and yeast cell. The "dsbandrepair" example in addition to the Belov and TLK models described above, provides another biological model the LEM IV model. The LEM IV model calculates cell survival based on the number of lethal damages that consider the induction of DSB and their spatial distribution. The fast and slow components of re-joining observed in experiments are related to the processing of simple and complex DSBs. In the "dsbandrepair" example each model is activated depending on the user.

3. Initial modelling of biological structures

To develop modelling of advanced biological structures in GEANT4-DNA, it is important to understand and analyse the methods and models previously used. Fig. 10 summarises the key developments spread across various track structure codes developed until 2016, which founded the basis for the current biological modelling. Further developments, providing a greater diversity in geometrical modelling, regarding the DNA and beyond the DNA level to the cellular level are discussed in section 4.

Initially, the structure of the DNA was investigated. Finch and Klug [69] presented the idea of the solenoidal structure of a chromatin fibre after observing the folding of nucleofilaments into supercoils under an electron microscope. They also used the idea of spacing between the turns of the solenoid rather than between the nucleosomes. This emphasised the need of histones for the stabilisation of the solenoidal DNA structure. Woodcock et al. [70] built upon the zig-zag model of the DNA structure, based on the initial folding step in the nucleosome packing forming a zig-zag ribbon which coils to form the double helix structure. Again, the importance of the histone for stabilisation was highlighted. The DNA model in the work of Charlton et al. [71] defined the DNA structure to differentiate between the base pairs and the sugar-phosphate back bone. Charlton et al. [71] used a central cylinder of 1 nm diameter to
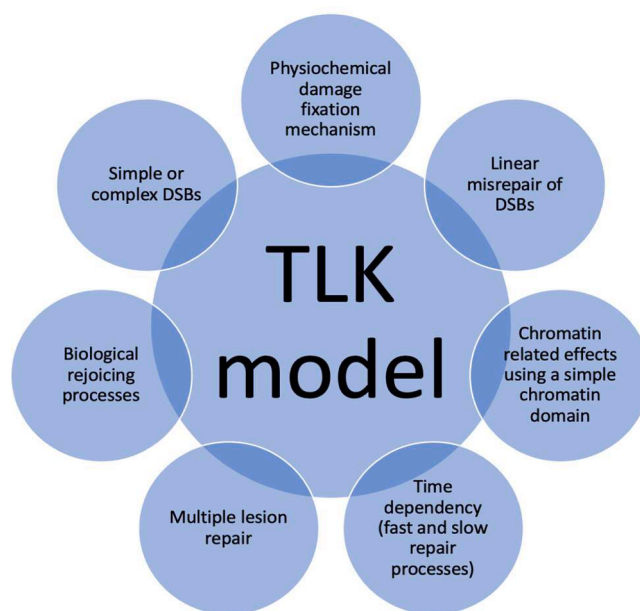
Fig. 9. Key assumptions, models and parameters used for the implementation of the TLK model based on Suzuki et al. [68] for the survival fraction modelling in GEANT4-DNA.

symbolise the base pairs, and half-cylinders, with a diameter of 2.3 nm and a width of 0.34 nm, as the sugar-phosphate back bone. Each model of the DNA abovementioned also described parameters such as packing ratio, pitch values and dimensions of the DNA as applicable. Nikjoo and Goodhead [9] investigated energy depositions in small sub-cellular targets represented by spheres or cylinders without any inner structure. These all concluded the dependence of biological damage on the structure of the DNA. Hence, special attention should be given to the modelling of the DNA structure for cell-specific models as cells not only biologically differ in their DNA compaction, but also this would influence the DNA damage quantification.

As biological advances in the knowledge of the DNA structure were made, more complex models were able to be created. Michalik and Begusova [72] proposed a model of a nucleosome consisting of a cylindrical histone of 6.52 nm diameter and 5.7 nm in length. The DNA double helix, formed of 200 bp (34 bp from the two DNA linkers and 166 bp from the DNA loops) with a diameter of 2.4 nm was wrapped around the histone with a pitch of 2.7 nm. Bernal and Liendo [73] used the quarter cylinder DNA structural geometry which was used to create the B-DNA conformation to evaluate direct damage. Peudon et al. [74] used the PDB to provide the structure of each DNA fragment (base, sugar-phosphate, or amino acid) that was taken from the nucleosome core particle 1AOI [75,76]. This geometry and their developed binary-encounter-Bethe, BEB, cross sections allowed to extend computations to amino acids constituent of histones to model accurately electron transport in chromatin via Monte Carlo simulations, and then DNA strand breaks. Bernal and Liendo [73] modelled 900 fragments of 30 nm chromatin fibres, containing a total of 500 nucleosomes. However, this model did not include the complete DNA content and hence highlighted the importance of base pair sequences to simulate realistic changes in genetic material.

Nikjoo and Girard [77] aimed to address the issue of incomplete DNA modelling by investigating different compaction levels: B-DNA double helix using the solenoid approach, nucleosomes, chromatin fibre loops and chromosomes territories to represent the complete genome of a spherically modelled cell nucleus containing approximately 6×10^9 bp. Friedland et al. [14] applied a similar approach in PARTRAC to model the whole genome of a fibroblast cell nucleus and a lymphocyte in their G0/G1 phase. This phase is used since the DNA density remains constant unlike in other cell cycle phases. The atomistic level approach was applied and arranged to form chromatin fibre loops. This geometrical approach created an unbroken sequence of DNA enabling the evaluation of DNA fragments. These studies emphasised that the complexity of biological analysis is dependent on the complexity of the geometrical model.

Incerti et al. [78] constructed DNA geometries directly in the GEANT4 application, starting with a simplified nucleus of 6×10^9 bp modelled by randomly oriented short segments of chromatin fibres. It was ensured that they do not overlap with neighbours based on the genetic dimensions proposed by Charlton et al. [71], as discussed earlier in this section. Between 2013 and 2015 several studies were occurring simultaneously to develop the geometries in GEANT4-DNA. Dos Santos et al. [55] used five compaction levels, namely DNA double helix, nucleosomes, chromatin fibres, chromatin fibre loops and chromosome territories to create ellipsoidal fibroblast and endothelium cell nuclei in the G0/G1 phase, as illustrated in Fig. 8a. The morphology of many cells were extensively investigated by the group to realise the dimensions of each nucleus. The relative volume of the DNA in the cell nucleus was calculated for each cell type, concluding the DNA is less compacted in the fibroblast than the endothelial cell used in the study. The chromatin fibre was
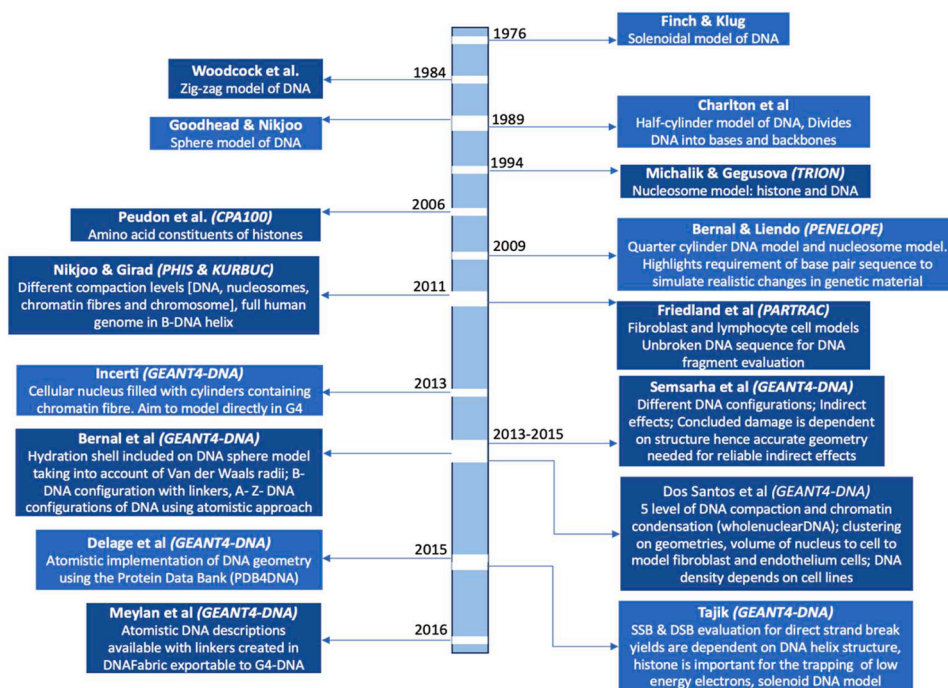

Fig. 10. Progresses of the initial modelling of biological structures in simulation from the DNA level to the cell level.

modelled by 90 nucleosomes, 31 nm in diameter and 161 nm in length. Each nucleosome consists of a cylindrical histone of 3.25 nm radius and 5.7 nm height, wrapped by 2 turns of DNA double helix. The DNA double helix contained 200 bp with an overall diameter of 2.16 nm and spheres of 0.34 nm representing the bases and backbone. Four pieces of chromatin fibre were assembled to form a diamond shape loop, which was used to full the chromosome territories. An additional compaction level inspired from a previous rosette-like structure was created from seven of the diamonds to form a flower shape used to fill the chromosome territories. Each nucleus was divided into 46 cubic regions with volumes proportional to the number of base pairs contained in it. There were filled uniformly to represent the number of base pairs per chromosome. The successful initial modelling of the whole DNA content of a specific cell was proposed as an advanced example in GEANT4, eventually implemented as the "wholeNuclearDNA" example. It was underlined in this study the dependence of the quantity and complexity of clustering increasing with DNA density, as the endothelium cell nucleus was always affected more than the fibroblast cell nucleus, despite change in particle or energy. Dos Santos et al. [79] additionally investigated the effects of chromatin condensation on direct DSBs comparing euchromatin and heterochromatin regions, decondensed and condensed respectively. They concluded that the condensed regions could be the location of more severe lesions in comparison to decondensed regions. They also investigated the effect of geometrical DNA description on nanodosimetric parameters using a cylindrical target volume representing 18×10^3 bp of DNA as a double helix DNA or randomly oriented cylinder approach [80–82]. Their work recommended the usage of thorough DNA geometry and scoring methods without fixed boundaries to analyse biologically relevant damage. All their analysis was carried out by evaluating clustering effects from the adapted DSBCAN algorithm. Bernal et al. [83,84] created the first, stand alone and publicly available procedure to allow the construction of an atomistic geometrical description of B-DNA. The analysis approach of the closest atom for an energy deposition was used to evaluate the biological damage. The atoms were represented as spheres and placed with corresponding Van der Waals radii. Later they expanded their B-DNA geometrical model to another two conformations, A- and Z-DNA. They observed a slight dependence on the DNA conformity and direct strand break yield. They also observed an increase in DBS yield with the packing ratio of the DNA double helix. Further work by Semsarha et al. [85–88], Bernal et al. [70], Tajik et al. [87] reinforced these findings by studying the effect on DNA damage with DNA conformation from different irradiation sources to investigate direct and indirect effects, comparisons with experimental data to investigate SSB and DSB and the role of histones in the DNA structure on DNA damage quantification. These studies highlighted the dependency of biological damage on the DNA conformation. The investigations regarding compaction and conformation indicated that the compaction and conformation of the DNA within a cell nucleus affects the DNA damage quantification and therefore an important consideration for cell-specific cell modelling.

Delage et al. [60] created a geometrical model based on the open source and free PDB. The PDB describes protein and nucleic acid structures including the atom coordinates, atom connectivity, and information about source of details. GEANT4-DNA successfully reads the PDB file and recreates the geometry to an atomistic scale. An external and open-source database enables the user to choose any model they desire for evaluation. The analysis method used is the closest atom in the DNA molecule approach to evaluate direct damage.

To encourage more accurate geometrical modelling, Meylan et al. [89] created a tool called DNAFabric, to easily adapt, visualise and modify geometries to account for different biological conditions. The models created in DNAFabric could then be exported into GEANT4-DNA and be used as targets. The tool initially investigated the compaction of a chromatin fibre and proposed to extend their models to multi-scale, molecular and cellular levels. The geometries created in DNAFabric have been successfully implemented in examples such as the "dnadamage1" and "dsbandrepair" examples in GEANT4-DNA.

After the initial geometrical modelling and definitions of DNA damage, several new geometries and advancements have aimed to help close the gap between physics, chemistry, and biology by providing more accurate biological modelling as well as evaluation of biological damage. The challenge in combining the principles and methods of these three fields into a coherent and accurate model remains. For example, while physics provides detailed descriptions of radiation interactions, translating these effects into biological outcomes, such as DNA damage, requires integrating chemical reactions and biological processes. Additionally, current models have shortfalls in the complexity needed to accurately represent biological systems, including the biological responses from radiation. The following section discusses the current models.

4. Advances in geometrical modelling

4.1. DNA level modelling

The "PDB4DNA" example and the "dnadamage1" example are currently available in GEANT4-DNA evolving the DNA level geometry. The "dnadamage1" example models a segment of chromatin fibre to analyse the direct and indirect damage. The "PDB4DNA" example, enables an interface to the PDB for the implementation of realistic molecular geometries and a variety of nucleosomes [60]. The "PDB4DNA" example has been explored using the standard '1ZZB' DNA model to investigate the direct and indirect effects of low energy [90] and quantification of DSBs [91] in addition to advancing to other models from the PDB, namely the '1BNA' model investigating the relative biological effectiveness from fast neutrons [92]. The "dnadamage1" example uses the DNAFabric tool, to create a 40 nm heterochromatin fibre with 18 nucleosomes and 19 linkers. Despite the use of the DNAFabric tool, "dnadamage1" example has not been used in many publications alone.

Further advances in DNA level modelling in GEANT4-DNA investigated the effect of chromatin compaction. Chromatin compaction plays a vital role in DNA repair. The compaction of the chromatin influences how the DNA interacts with radiation and hence influences the sensitivity to DNA damage and the yields of DSBs [93–98]. Most cells modelled before 2019 were without any euchromatin contribution or differentiation between regions of heterochromatin and euchromatin of a cell nucleus.

Tang et al. [99] investigated the effect of chromatin compaction DNA damage by modelling a fibroblast cell filled with either heterochromatin or euchromatin only, and an endothelial cell filled with heterochromatin only or a uniform distribution of 42 % heterochromatin and the remaining of euchromatin. The DNA damage evaluation investigated the proportion of direct and indirect damage. Each cell model used the DNAFabric tool and the whole human genome in the G0/G1 cycle phase. Radiobiological studies provided the dimensions and volume for each cell type. DNAFabric models a cell nucleus in three steps. First, 46 chromosomes are placed in a condensed form. These condensed forms are then expanded, using a space filling algorithm, generating DNA loops within each domain ensuring a continuous chromosomal territory [100]. A compilation of 20 nucleotide pairs created a B-DNA double helix which was wrapped around a histone protein to create a nucleosome. 23 nucleosomes are rotated in the Z-direction to create the chromatin fibre which is connected by nucleosome linkers. The chromatin fibres were then compacted into five different voxels (straight, right, left, up and down) representing different compactions of the chromatin fibre. These chromatin voxels are then contained into domains, representing human chromosomes, where the chromatin domains are spheres with a radius of 500 nm containing approximately 1 million pairs of nucleotides. Tang et al. [99] concluded that the damage on the genome is dependent on chromatin compaction and damage occurs to both the euchromatin and heterochromatin regions. They also observed an increase in indirect damage in the euchromatin compared to the heterochromatin initiating a possibility of increasing radiosensitivity. The increase in indirect effects on the euchromatin can be explained by the euchromatin being more hydrated and has a lower concentration of histones [101]. Non-histone proteins were not modelled in the geometry directly, however the scavenging effects of radicals by non-histone proteins were considered through different parameters.

The DNAFabric tool was enhanced by Thibaut et al. [102]. They modelled a new endothelial cell nucleus in the G0/G1 phase based on the isochore theory, to investigate the need of accurate chromatin compaction for radiation damage investigations. The isochore theory defines the heterochromatin and euchromatin compaction distributed along the genome according to five different families (L1, L2, H1, H2 and H3), each with a different heterochromatin to euchromatin ratio related to their compaction level. For this cell, 48 % of the nuclei was modelled as the heterochromatin and the rest was modelled as the euchromatin voxels. The isochore mapping [103] and the human reference sequence (GRCh38- fully mapped genome in the form of FASTA files) [104,105] were also required to create this geometry. A 6–10 % increase in DSB yield was observed by the organisation of the chromatin fibres in different compaction levels. It was further identified that the genome core (H2 and /H3 families – mostly euchromatin) was more radiosensitive than the genome desert (L1, L2 and H1 families). Thibaut et al. [102] also observed their isochore geometry to have a higher mean number of indirect strand breaks in comparison to similar numbers of direct strand breaks over a range of energies. These simulation differences would translate into more significant biological effects. Again, this highlighted the need for accurate DNA geometry which can only be successful if advanced biological analysis accompanies it. This particularly creates interest for investigations of biological repair pathways on highly detailed nuclear geometry.

As an alternative to the DNAFabric tool, investigations on the chromosome territory-interchromatin compartment (CT-IC) were used to model the DNA. Lee and Wang [106] investigated DNA DSB yield by introducing the CT-IC geometrical modelling for the nucleus. Their DNA model was used to present a cell-by-cell simulation integrating GEANT4-DNA and sub-nuclear structures to quantify biological damage. The model highlights the uneven distribution of chromatin domains and interchromatin compartment with a chromatin compaction to be of a 22:1 ratio. This is due to each chromosome occupying distinct chromosomal territories during the interphase, which are comprised of a multitude of chromatin domains containing the bead like structures. The bead-like structure is comprised of 30 nm diameter chromatin fibres. To apply this model, firstly, a data library containing detailed track structure co-ordinates (PTSC) for various particle types, energy and doses using GEANT4-DNA was created. Additionally, a cell nucleus dataset library was used which contained detailed chromatin fibre locations for many cells. The use of such a database makes implementation of multiple cell-specific modelling more easily incorporable through this modelling approach. The PTSC is then mapped and overlaid with the cell nucleus to produce DNA DSBs on a cell-by-cell basis. The sphere packing algorithm packs 6000 chromatin domains of 400 nm diameter into a spherical cell nucleus of 11 μm in diameter. The damage analysis was carried out using a clustering algorithm, by applying alternative biological quantification suitable for this model. However, the authors emphasised the intermediate complexity of this model due to the lack of molecular detail and fine resolution on their DNA structures.

Ingram et al. [107] used the modelling approach initiated by Lee and Wang [106] to study cellular radiosensitivity in different cell types by using different genome organisations for different cells to quantify DNA damage. They used information about the chromosome structure in the form of Hi-C data, a genomic analysis technique which averages the result of a large cell population [108]. This data is implemented into GEANT4-DNA by a python-based code called nuclear organisation modelling environment (G-NOME). Three cell types, namely human foetal lung fibroblast (IMR90), human adult mammary epithelial (HMEC), and human B-lymphocyte (GM12878) were created containing 6×10^9 bp. The varying chromosomal connections within different cell types are shown to be essential for differences in cellular radiosensitivity. Difference in shapes, spherical and ellipsoidal, and inclusion of Lamina-associated domains (LADs) were created to analyse the effect of DNA conformation. Similar to Lee and Wang [106], a bead-like structure is defined by topologically associated domains (TADs). Each bead produced by G-NOME is placed as a spherical geometry in GEANT4 to implement the geometry in GEANT4-DNA. However, the analysis and controls are based in their DNA damage application [109,110]. Ingram et al. [107] observed that changes in either the cell-type, addition of LADs and changes to the shape do not have noticeable influences on the yields of DSB and SSB DNA damage. However, differences were observed in the pattern of damage. They also observed changes in inter/intra chromosomal DSB clustering which may be a predictor of inter- and intra-chromosomal misrepair, which would result in differing biological responses. This modelling approach is already included in the TOPAS-NBio, an extension of TOPAS, layered on top of the GEANT4 MC toolkit [111]. This modelling approach could be expanded to include the nucleosomes rather than cylinders in the beads and be more representative of euchromatin and heterochromatin regions. This method of DNA conformational modelling can be used to model different cell sub-types and cell-cycle specific states in addition to different cell types,

solely based on the differences in chromatin conformation. Hence, modelling according to the genome organisations has great potential to advance cell-specific modelling. For DNA level modelling in particular, the inclusion of the effect of different repair pathways with the differences in chromatin conformation should reflect behaviour such as proliferation rate of each cell type.

To summarise, the DNA level modelling has been advanced to include the euchromatin and heterochromatin regions of the nucleus. The DNAFabric tool has been used to model different cell types with accurate DNA level modelling. However, this requires expertise in an external software to create the model and then import it into GEANT4-DNA. Alternatively, CT-IC is based on databases, such as the "PDB4DNA" example in GEANT4-DNA. The inclusion of databases provides an easier method to implement a variety of nuclei. This methodology can also be advanced to consider different geometries alternative to cylinders. This would also help to consider heterochromatin and euchromatin nature, thus advancing the model. To date, there are no investigations on the different combinations of base pairs and the effect this has on the DNA damage. Since different base pair sequences require different energies for DNA damage, accounted for in GEANT4, this could provide a novel method in geometrical modelling to create cell-specific geometry at the DNA level. Advancements in the geometrical models would also require cooperative physics models to be compatible with such geometrical advances.

4.2. Cellular level modelling

The "clustering", "wholenuclearDNA", "microbeam", "molecularDNA" and "dsbandrepair" examples focused on creating cell geometries in GEANT4-DNA. The "dsbandrepair" example is part of the advanced examples in GEANT4-DNA whereas the "microbeam" example also provides a novel approach to model a cell, however, is included within GEANT4 only. The "clustering" example enables the evaluation of SSBs, DSBs and complex SSBs due to direct damage using the clustering algorithm. The default model is of a target box; however, this can be altered to mimic a cell like geometry.

The "wholenuclearDNA" example [55] uses the clustering algorithm to calculate the direct, indirect and mixed DSBs. This example models a complex fibroblast cell which represents the nucleus of a single human cell using the complete human genome in the G0/G1 phase of the cell cycle with a total of 6×10^9 bp. The morphology of the ellipsoid axes and the volumes were experimentally obtained. The nucleus is based on the CT-IC model using five different levels of compaction to creating "rosettes" from the DNA double helix model [100]. The five compaction levels are the DNA double helix, nucleosomes, chromatin fibres, chromatin fibre loops and chromosome territories. These are subsequently placed in chromosome territories with volumes proportional to the number of base pairs composing the chromosome. The DNA composition in the nucleus is based on the atomistic approach where six molecules, four for the bases and two for the sugar-phosphate backbone. This cell model also includes the cell nucleus and cytoplasm, where the volume of the nucleus is about a quarter of the whole cell volume [112]. This is modelled solely using GEANT4-DNA while still maintaining accurate DNA density, biological relevance, and similar results for DNA damage to relevant published studies. The authors of this example analysed the effect of DNA density on clustered damage at different energies by modelling an endothelial cell for comparison with the fibroblast cell, where the volumes of the fibroblast and endothelial are 732 μm³ and 219 μm³, respectively. They observed an increase of the total number of complex DNA damages in the endothelium cell nucleus due to the increase of DNA density in that nucleus. It can therefore be concluded that there is a dependence of DNA density and cell type to direct DNA clustered damages and hence damage repair. Limitations of this example include the evaluation of only direct damages due to a limited implementation of chemistry and physics models at the time of publication to account for indirect effects. There is also limited experimental data to assess the influence of DNA density and hence limited publications using this geometrical approach.

The "microbeam" example provides a cell geometry by using confocal microscopy images of a fibroblast cell [113]. The nucleus of the fibroblast cell was stained using the fluorescent H2B-GFP protein, and the cytoplasm was marked with propidium iodide, an RNA and DNA marker. The propidium iodide is also able to locate the nuclear regions highly rich in RNA protein and heterochromatin inside the cell's nucleus. Images were obtained using a Leica DMR TCS SP2 confocal microscope for several two-dimensional resolutions, up to 512×512 pixels. This stack of images was then reconstructed to create a 3D model using the Leica Confocal Software. These images were transferred into the Mercury Computer Systems, Inc., Amiraw, for filtering and geometry reconstruction [114]. Filtering was necessary to eliminate the residual fluorescence generated by the cell glass support used for microscopy. An image reconstruction methodology provides information about the total number of voxels for each cellular region (cytoplasm, nucleus, and nucleoli) and their dimensions. The confocal data is imported into GEANT4 by a list of each voxel's position, material composition and fluorescence intensity content for the construction of the geometry in GEANT4. This example has a huge potential in GEANT4-DNA since the elemental mineral composition is also included and is calculated using the GUPIX software [115] for the nuclear and cytoplasmic areas. This can be used to evaluate the effect of a realistic cell composition rather than solely of water. Furthermore, this modelling method can be used to create realistic 3D and multi-cellular phantoms of biological tissues and even organ sub-volumes. Despite this geometrical approach requiring extensive image reconstruction tools, Arnaud et al. [116] created an A-431 cell geometry to explore the effect of source distribution with the Auger emitter iodine 125 for radioimmunotherapy. Using a similar geometrical modelling approach as in the "microbeam" example, they concluded the cell geometry, as well as the radionuclide distribution can change the whole energy deposition in a whole cell or nucleus, especially for short range particles. Key differences were observed between positioning the source at the cell surface and targeting the nucleus. These alterations caused fewer damages to be registered in the nucleus for the spherical model, as low energy electrons could not reach the nucleus, however when an electron does reach the nucleus, more energy is deposited.

To advance the cell-based geometry the DNAFabric tool has been used. Meylan et al. [46] modelled a human fibroblast in the G0/G1 phase of approximately 6.4×10^9 bp of nucleotides. The overall cell geometry is given as an ellipsoidal, with the same three step methodology regarding the condensed DNA placement and expansion into the volume of the nucleus as described in section 4.1.

Sakata et al. [50] used a similar modelling approach to enhance the fibroblast model by creating a fractal cell nucleus. This helped to create a continuous chromatin segment by iterating a Hilbert curve as a fractal 8 times providing a 0.012 bp/nm^3 DNA density in comparison to the 0.015 bp/nm^3 DNA density used by Meylan et al. [46]. The chromatin voxels which fell outside the Hilbert curve were not included in the geometry. This geometry has been used to investigate the IRT methods introduced into GEANT4-DNA to compute the diffusion of the radiolytic products. Sakata et al. [64] modelled a cell geometry, using the fractal geometry method, by immersing the cell nucleus into the cytoplasm which was all surrounded by the cell membrane. This was created by including a 1 mm thick water absorber covering the cell nucleus, just before the cell geometry, acting as cytoplasm to mimic the T25 cell culture flask. Based on the cell nucleus geometry of Sakata et al. [50], a cell model was created where the nucleic volume of approximately 528 μm^3 containing 6×10^9 bp and a cell volume of 2052 μm^3 was used. The remaining cell was filled with water to model the cytoplasm. The authors observed the geometrical parametric improvement to not have much influence on the DSB yields. However, turning off the histone scavenging effect created a decrease of the SSB to DSB ratio yield. This initiated the idea that the histone scavenging has a role in protecting against radiation-induced DSBs. They highlighted the need for several additional parameters for modelling other cells beyond geometry including the mechanisms of radiation-induced DNA damage. Shin et al. [117] created a human fibroblast cell which was used in the "molecularDNA" example. They used three segmented models, straight, turned, and turned-twisted to create inter-linked chromatin segments.

The "molecularDNA" example offers three different targets: cylinders, E. coli and human cell based on previous prototypes [33,45, 50,118–120]. The authors not only advanced the human fibroblast model but also included the latest approach to model the chemical stage. Each of these biological targets contained different base pair densities to be biologically representative. The chemical advancements use the synchronous IRT model and implements the G4EmDNAChemistry_option3 chemistry list based on Plante and Devroye [40], hence direct and indirect damage can be calculated, where direct damage is associated with a strand molecule, or a base molecule and an indirect damage is classified when a chemical reaction leads to a strand break. Additionally, an upgrade of computational tools to estimate DDR such as repair kinetics and survival probability of cells has also been implemented. This example expands the damage classification adding further complexity of damage in addition to the source of damage. Further detail about this example can be found elsewhere [22]. More recently, Chatzipapas et al. [121] advanced the "molecularDNA" example with new cell geometries for investigating DNA damage and response from helium beams. The authors modelled HTB-177 and MCF7 cells based on the default human cell geometry available. The information used for these models were acquired from morphometric experimental data [122]. They changed the voxel size for both cell types to contain 38 nucleosomes to give a base pair density of approximately 0.011 bp/nm^3 and 0.017 bp/nm^3 for the HTB-177 and MCF7 cell lines respectively. The lack of modelled difference between the two cell lines could indicate the external cell geometry is not enough for cell-specific modelling or radiosensitivity analysis. Therefore, differences in cells from the cell shape to the DNA, should be included in the future. The models in this example also create a geometry for the cell and nucleus only, not the chemical composition of the cytoplasm nor the sub-cellular structures.

Wang et al. [123] provides an interesting alternative to using DNAFabric. The authors modelled six different cell lines; using mesh-type modelling obtained from fluorescence tomography. This modelling technique was investigated for the PHITS and GATE Monte Carlo codes and has started in GEANT4-DNA to model the mitochondria networks, described in more detail in section 4.3. The methodology introduced by Wang et al. [123] can be used directly in GEANT4-DNA. It can also help in providing accurate cell geometrical modelling from the DNA to the cellular level. It can also be easily expanded for multiple cells and cell populations.

The "dsbandrepair" example furthers the cell-specific modelling approach in examples in GEANT4-DNA by considering euchromatin and heterochromatin regions. Unlike the "molecularDNA" example which is modelled using python, "dsbandrepair" uses DNAFabric to create the heterochromatin and euchromatin regions of a human fibroblast, human endothelium and Saccharomyces Cerevisiae yeast cell. The heterochromatin and euchromatin regions are determined using experimental data. This example is coupled with the ability to apply repair models for extensive biological damage analysis in GEANT4-DNA.

To summarise, different cellular geometries, which lacked enough distinction between them, do not greatly affect the yields of SSBs and DSBs. This is consistent with observations of a near-constant DSB yield rates across many cell types. This indicates that the effect of cell geometry does not seem to be the only crucial parameter to investigate. The DNA level and DNA compaction should still be taken into consideration in addition to the external cell geometrical modelling. The lack of distinction also arises from the lack of modelling beyond the nucleus, as highlighted by the "microbeam" example, where the inclusion of the chemical composition can greatly affect the energy deposition. Methods such as the mesh-type modelling and the use of databases for the chromatin compaction are both plausible methods with great potential to model specifically cells all within GEANT4 itself.

4.3. New biological structure level modelling

Taheri et al. [124] provide an extensive review on the advances on nanoparticle radiosensitisation modelling with the GEANT4-DNA toolkit. Nanoparticles have been modelled using GEANT4-DNA outside the cell membrane, within the whole cell, inside the cytoplasm both distributed and around the nucleus and inside the nucleus only. Although nanoparticles are not biological structures themselves, Taheri et al. [124] suggested the need for more complex structures of human cells, including organelles in addition to the modelling of DNA damage, repair processes and chemical reactions over longer timescales to understand the effects of nanoparticles at the biological scale in GEANT4-DNA. This section describes geometrical modelling of biological structures beyond the nucleus and cell, such as the E.Coli structure presented in the "molecularDNA" example. E.Coli is of interest in the radiobiological field due to the striking similarities this particular bacterial variation has to mutational changes in higher plants and animals [125]. Lampe et al. [45] created an E.Coli bacterial cell using the space-filling Hilbert curve approach. Straight and rotated DNA segments were modelled containing the structure of B-DNA. This geometry was packed into an ellipsoid, for which the Hilbert curve was iterated 4

times, and 3 Hilbert curves were placed end to end to fill the entire cellular ellipsoid. Again, voxel regions outside the defined nucleus region were not considered providing a 4.63×10^6 bp E.Coli structure, keeping the model mostly connected.

Belov et al. [126] modelled a neural network containing 10 cells, reconstructed from NeuroMorpho.org repository [127], as implemented in the "neuron" example. The 3D neuron model is made of cylindrical segments for the dendrites and spherical segments for the soma to complete the neuron. Alongside providing a new application in the GEANT4-DNA toolkit, the cell morphology was also concluded to be a determining factor in neuronal radiation injury. Bayarchimeg et al. [128] developed a NEURON application to investigate the effects of radiation on the central nervous system. The toolkit reads any standardised neuromorphometric format (SWC) file [104] representing the neuron morphology and is modelled based on the work by Belov et al. [126]. The SWC files describe 3D coordinates of a neuron morphology. The multiple cell modelling promotes the ability of GEANT4-DNA to model populations of cells rather than single cells.

The effect of sub-cellular targets driving radiosensitivity beyond the DNA in the nucleus is sparsely studied, in comparison to the DNA. Mitochondria are responsible for key functions such as metabolism and reactive species production. They are the only extra-nuclear material containing genetic material; however, they lack functional DNA repair [129]. McMahon et al. [130] was the first to model the mitochondria as a target when investigating the effect of mitochondria for radiosensitisation by gold nanoparticles. This provided information on the physical dose distribution at the sub-cellular scale. In GEANT4-DNA, 30 elliptical mitochondria were randomly distributed and orientated in the cytoplasm of a cell with a nucleus. The estimation of DNA damage was representative of the degree of the clustering ionisations. A threefold factor increase was observed in the number of ionising events to the cell irrespective of the inclusion of nanoparticles and energy of X-ray. However, a much smaller impact on ionisation clustering was observed within the nucleus. This meant that DNA was subject to significantly more radiosensitisation in mitochondria than within the nuclear volume. The mitochondria have become of increasing interest due to their role in cell survival. Zein [131] created a more complicated model by utilising the G4TessellatedSolid class in GEANT4 enabling complex and irregular solids to be defined by a surface mesh, with the implementation of CAD based geometries importable directly into GEANT4 by CADMesh [132]. The mitochondrial phantom investigated by Zein [131] was modelled from staining the tracks of mitochondrial networks' continuous remodelling. Zein [131] converted the 2D slices into 3D objects as STL file formats using Imaris creating a mesh geometry in GEANT4 from the STL files [133]. Most importantly, Zein [131] described a new method for building phantoms from microscopic images. Tavakoli et al. [134] used a mathematical algorithm for geometrical construction to create a model for the circular mt-DNA, containing approximately 17,000 bp. Later this methodology was expanded to create a geometrical nucleotide resolution model of supercoiled mt-DNA, also containing approximately 17,000 bp. These geometries were created to perform realistic evaluations of DNA free radical reactions. The latter geometry includes two semicircles and spiral paths between them, creating the SmtDNA tool.

Kondo et al. [135] created a pUC19 plasmid geometry with 2686 bp in a buffered solution of DMSO. Plasmid DNA can be found in three different conformations (supercoiled, open circular, and linear) representative of DNA damage (no damage, SSB and DSB) [136]. Through gel electrophoresis, the intensity of the three DNA damage classifications can be quantified. The simulation took into consideration DNA concentration, dosage, DMSO and plasmid supercoiling. The latter was measured using the super helix density value used in a Brownian dynamics plasmid generation algorithm [137,138]. The plasmid was deformed into a 179-sided polygon, where each side contained 14–15 bp. Algorithms were used to create the coiling of the plasmid using the DNAFabric tool. These geometries helped to validate the IRT models emerging in GEANT4-DNA to include water radiolysis in GEANT4-DNA simulation.

This sub-section uses the geometrical modelling techniques used for the nucleus and cell modelling to model beyond the DNA and nucleus. Sub-cellular structures and their effect and role in biological response from ionising irradiation is a field yet to be fully understood. The use of databases, mesh-based modelling, and tools such as the DNAFabric tool to create such different structures reinforces the reliability of these modelling methods to create any specific biological structure desired by a user.

4.4. Cell population modelling

As the DNA, cellular and sub-cellular modelling are evolving in GEANT4-DNA, it is vital to remember the aim of simulations. The aim of simulations is to model as accurately as possible the experimental procedure to obtain comparable results between the two. Cells are not irradiated as a single cell, hence modelling multicellular populations are more representative of radiobiological studies. Populations and multicellular populations also can change the behaviour of a given cell and hence its biological damage response. The following section provides summaries and relevance of brief studies which used multicellular modelling.

Forster et al. [139] used a multicellular tumour of head and neck squamous cell carcinomas (HNSCC) to model pO_2-dependent DNA damage for chromosome aberrations and cell killing from misjoining. The authors filled a volume of 0.2 mm^3 with 1224 non-overlapping cells of 1.53×10^8 cells/cm^3 density using algorithms described previously by Forster et al. [140]. To be representative of FaDu HNSCC cells, cell volumes of 1437 μm^3 to 2053 μm^3 were used, where the nucleus occupied 8 % of the cellular volume. As an application for the new stochastic model proposed, the voxelised tumour was replicated 125 times to form a cubic volume of 1 mm^3, generating a connected network of blood vessel through 1 mm^3 tumour. They concluded that other mechanisms, beyond misrejoinings involving DSBs may be important. Although the authors used the geometry to test their stochastic model, they provided insight of multicellular modelling. Similarly, Tamborino et al. [141] used multicellular modelling to evaluate the early radiation DNA damage occurring during 177Lu-DOTATATE radionuclide therapy by using both polygonal mesh models from representative confocal microscopic images defining the nucleus, cytoplasm and gogli apparatus. These cells were copied to create a cell population.

Liu et al. [142] created a computational multicellular system using a python-based C++ code, accompanied by GEANT4-DNA for the radiation transport to obtain the dose and DSB yield. This idea was based on the need to represent 2D, or 3D models of cell culture

used in radiobiological studies. Their multicellular simulation included spherical cells with both nucleus and cytoplasm compartments. The cytoplasm was treated as representative of all other cellular organelles inside it; however, all were modelled with liquid water material. Meshed grids were used to create the 3D layout by stacking multiple layers of 2D monolayer grid without cells overlapping each other, providing a total of 1000 cells. These were then randomly distributed inside the cell culture model. The final geometry can be imported into GEANT4 for the radiation transport. The authors conveyed guidelines for creating a thorough toolset for simulating DNA damage and cellular dosage in multicellular tissue systems. Additional experimental research is required for rigorous validation and benchmarking to assess the performance of the proposed model thoroughly.

Salim and Taherparvar [143] used multicellular modelling, previously described by Oliver et al. [144], who modelled cells as two concentric spheres. One representing the nucleus and the other sphere mimicking cytoplasmic regions using typical values of a cell from literature (compartment sizes, elemental compositions, and number densities).

Another approach was described by Salim and Taherparvar [143] used a hexagonal packing approach and split the model into 3 layers, where the central cell is surrounded by 12 others with nucleic and cell dimensions typical for lymphocytes and V79 Chinese hamster cells and intercellular spacing. These are embedded in a larger sphere representing the extracellular matrix with a density of soft tissue. The study was used to in the Medical Internal Radiation Dose (MIRD) tool. The authors concluded the presence of cytoplasm, extracellular matrix and surrounding cells can affect the nuclear dose by up to 13 %. Additionally, they reinforced the effect of cell and nuclei sizes on the dose [143].

Methods to model cell populations have been introduced in this sub-section including both the use of external tools and capabilities within GEANT4. Advantages and disadvantages of each method have been briefly discussed including some models considering different sizes of cells within the same cell population to the lack chemical composition and DNA level geometry. This has indicated a vast number of options for a user to model cell populations. However, to be representative of radiobiological studies, populations, and cell-to-cell interactions within these populations should be accounted for and hence such models also require adequate biological damage analysis and physical models based on the numerous biological damage outcomes from a cell population.

5. Co-operative platforms with GEANT4-DNA

Beyond its stand-alone use, GEANT4-DNA has also been involved in the creation of co-operative platforms to enhance the development of biology in GEANT4-DNA. These platforms address current gaps in GEANT4-DNA by looking at the subcellular and multicellular geometrical modelling. They also create alternative biological damage analysis approaches to account for the changes in their geometry. Six such co-operative platforms are described in the following sub-sections.

5.1. Radiation damage to biomolecules (RADAMOL)

RADAMOL is an extension of the previously created RADACK model investigating radical attack to biomolecules [145,146]. To evaluate DNA radiation damage caused by electrons, protons, and alpha particles, the RADAMOL simulation programme was initially created in 2014. Its primary focus was on the impact of charge migration and scavenger concentration on DNA damage quality [147]. In such simulations, electron and hole migration along the DNA macromolecule was considered for the first time in 2014. The static geometrical models used the PDB format to provide atomistic details of a free DNA oligomer or DNA in a complex with a lac repressor protein. The distribution of primary biomolecular damage was analysed by investigating radiation type, energy, oxygen content, and DNA interaction with proteins. As a result, RADAMOL can examine how radiation harm affects various intracellular functions and subcellular structures. The study of subcellular structures is becoming increasingly crucial to comprehend how radiation affects DNA and how to most effectively treat individual cancers.

5.2. CompuCell3D (CC3D)

Lui et al. [148] presented CC3D as a platform that facilitates multi-cell-based models alongside the evaluation of how radiation affects the biology of a living tissue, considering the effect of time. CC3D has been extensively used to model tumour characteristics such as vascular tumour angiogenesis [149]. To model vascular tumour angiogenesis, different cell types such as necrotic, endothelial, proliferating tumour and neovascular endothelial cells and extracellular matrix (ECM) are used to model a vascular tumour undergoing microbeam radiation treatment. The spatial size of the spheroid model was ensured to match the spatial scale of the radiation beam, such as in the "microbeam" example in GEANT4. To link the two platforms successfully, the RADCELL module was used [149]. Tumour cellular geometry created in CC3D was translated into GEANT4 by RADCELL, which also provided information about the cell dose and DNA damage to CC3D, updating the cell characteristics with time, during GEANT4 simulations. CC3D includes various cell biology modelling, including cell growth and mitosis, cell-cell adhesion, and vascular endothelial growth factor (VEGF) signalling process. The use of an additional platform to GEANT4 enables identical simulations to be carried out to compare the effects of tumour growth and morphology without the effect of irradiation.

Biological effects from ionising irradiation have been established to be highly complex mechanisms involving multiple processes at different spatial and temporal scales. CC3D enables the study of both a single cell and entire tissue at the same time and models the effect of time on biological damage. The authors of CC3D use a 'cell state transition model' which quantifies the temporal transition of the possible cell phenotypes after irradiation through three major cell states, which are dependent on the cell-cycle: healthy, arrested, and dead. Through python code, based on simplified wrapper and interface generator (SWIG), cell dose and damage are quantified to determine the cell transitions for CC3D cells [150,151]. The macroscopic behaviour of cells according to cell transition state were

determined by DSBs and glucose concentration and not linked to intracellular responses. Lui et al. [148] proposed the use of repair pathways to be included in the intracellular simulation functionality. However, this requires estimating cell parameters from measurable data or theoretical values.

It is evident that this extensive modelling platform can be used to examine how radiotherapy would be delivered to such a complex tumour involving vascularity, a common occurrence in malignant solid tumours. Moreover, this potential to expand models to other complex 3D cell cultures in GEANT4, will broaden the interpretation of radiation damage in complex biological structures. Although detailed geometrical modelling at the cellular and DNA level is yet to be implemented in this example, since the aforementioned study, an investigation of radiation-induced gastrulation failure of chick embryo has been carried out [152].

5.3. Cell population (CPOP)

CPOP, is an open-source C++ population modeler created by Maigne et al. [153] for radiobiological applications, with the ability to model 2D and 3D realistic cell populations. CPOP can represent enormous 3D cell populations by using force law systems to control cell-cell interactions and independent deformable cells that are specified with their nucleus, cytoplasm, and membranes. Pairing CPOP with GEANT4 facilitated the investigation of energy depositions throughout cells to investigate radiation outcomes using high-Z nanoparticles.

CPOP is separated into two primary libraries: the Multi Agent System (MAS) library, which involves the 'Agent' family class, which is the cell interactions within the population, and the "Modeler" library, which uses meshes to model cell geometry. This Modeler contains two family classes 'geometry' and 'models' corresponding to the geometry of each cell and the model chosen to create it. Each cell is accompanied by comprehensive parameters: nucleus radius, cell membrane radius, forces, cytoplasm, nucleoplasm materials, direction, orientation, and speed. The geometry can be transferred into GEANT4 toolkit by a generation of an XML file or simulating GEANT4 energy depositions through CPOP, for which the energy depositions are automatically calculated and allocated to cell population geometry in the XML file. After compilation, CPOP can initiate GEANT4 simulations because it has a complete interface with the GEANT4 Monte Carlo toolkit.

The geometrical model presented in the introduction to CPOP was based on the realistic 3D cell population of SK-MEL28 melanoma with dimensions of the spheroid diameter, spheroid population, cell diameter and nucleus diameter defined. The regions of energy depositions were defined across three virtual layers corresponding to the layers of the spheroid by radius: necrosis, intermediary and external. This enables users to fix their own parameters including force law system definitions for cell-to-cell interactions. The experimental comparison was obtained from X-RAD 320 Biological irradiator generating orthovoltage x-rays while investigating gadolinium nanoparticles present in the spheroid.

A key advantage of this platform over CC3D is the ability to obtain deformable cell shapes with dynamic radii, agreeable with experimental outcomes. These are created using meshes to warp each cell creating deformable cells, using a dynamic radius to obtain a high-level conformation of cell membranes and their neighbours. Unlike CC3D, which models population growth, CPOP represents a final state of desired cell number as observed with microscopy and can create multicellular spheroids with a population of over one million cells using the Computational Geometry Algorithms Library (CGAL) [154]. The combination with GEANT4 addresses the need of 3D cell culture modelling in GEANT4 which currently just investigates 2D cell culture models. The creators of CPOP proposed to further expand this work by integrating DNA geometrical models into cell nuclei and using GEANT4-DNA physics and modelling to evaluate biological damage.

5.4. DNA damage response to ionising radiation (IDDRRA)

IDDRRA presented by Chatzipapas et al. [155] focuses on providing DNA models of any base sequence and geometry defined by mathematical functions in python to be modelled within minutes in several positions and orientations, with an integrated graphical user interface (GUI). They also developed algorithms to analyse the direct DNA damage, namely DSB, SSB, clustered strand breaks in addition to the probability of repair. The future of this work aims to include more detailed repair models and indirect effects from irradiation.

5.5. MINAS TIRITH

The MINAS TIRITH tool was developed by Thibait et al. [156] for simulating radiation-induced DNA damage at the cell population level. The method was based on databases of GEANT4-DNA microdosimetric parameters and DNA damage distributions. Thibait et al. [156] presented a cell population of 200,000 cells with a single nucleus geometry, of approximately 6×10^9 bp represented by an elliptical cylinder, representative of an endothelial cell type.

In this tool the geometry is used to assign certain microdosimetric parameters for the dose and damage considerations. A specific energy is defined to each cell in the population modelled for a particular absorbed dose. Each cell is then assigned a realistic number of DNA damage based on the specific energy retaining consideration of the stochastic nature of their occurrence. Since the MINAS TIRITH only takes account of the variability of cellular responses associated with the distribution of energy deposition and excludes other types of individual variability or the heterogeneity of cell nucleus shape (geometry or volume) within the cell population, a microdosimetry formalism was employed.

Unlike the other software's, the MINAS TIRITH tool has made use of the GEANT4-DNA extension of the GEANT4 toolkit and works towards reducing computational time due to complicated geometry. The authors also highlighted the comparisons of the MINAS

TIRITH tool endothelial cells with the GEANT4-DNA fibroblast cells as a reference. This has also been previously highlighted in the work of Sakata et al. [157] where experimental data is compared to that of a different cell type in Monte Carlo modelling. This is a key indicator for the need for cell-specific modelling to the DNA level in simulation work. The authors proposed to increase comparisons with experimental data obtained from cell populations and validate their tool further by comparisons with foci and DSBs. However, it does assume several things regarding the modelled geometry: fixed time point of cells, detailed DNA geometry, a single size nucleus and cell size despite cells in a population not being all the same dimensions.

5.6. TOPAS-nBio

TOPAS-nBio [158] is an extension of the original TOPAS project which focuses on physico-chemical simulations at the nanoscopic and microscopic scales. The specific objective of this project was to create a flexible and easy-to-use platform to run GEANT4 simulations for users without solid programming training. GEANT4 requires the user to build their own applications, having to implement, compile, and debug a few C++ classes. TOPAS and TOPAS-nBio work using text files in which parameters are as user-controllable as possible, covering a long range of applications and preventing the inexpert user from creating their own code. In TOPAS-nBio, DNA molecules are represented as volume models, meaning their molecular or atomic composition is omitted. The DNA model follows a double-helix structure in which each nucleotide is composed of two volumes, a nitrogenous base, and a sugar-phosphate backbone. Different elementary volumes can represent these moieties, such as half-cylinders, cylinder sectors, or spheres. An additional volume representing the neighbour hydration layer surrounds the backbone volumes.

The TOPAS-nBio collaboration included three distinct types of damages that can be inferred from the physical, physicochemical, and chemical stages of GEANT4 simulations. First, direct damage is considered by the accumulation of energy deposits in the volumes representing bases and sugar-phosphate backbones, assuming a damaged structure when a given threshold is exceeded. Second, indirect damage is mediated by the diffusion and reaction of radicals produced after water radiolysis. As TOPAS-nBio lacks the molecular composition of each base pair in the DNA double-helix, a stochastic approach is utilised, selecting randomly whether a volume is damaged by a radical entering into it according to a given probability fixed by the user. Third, quasi-direct damage is the charge transfer that happens at the physical stage whenever a water molecule in the proximities (up to 11–13 water molecules) of the DNA molecule is ionised [159,160]. This charge transfer can induce damage in each moiety of the nucleotides, with a probability controlled by the user in TOPAS-nBio. As shown by Bertolet et al. [161], whenever volume models are utilised, the parameters to control when direct, indirect, and quasi-direct damage happens as a function of physicochemical events need to be tailored to each specific geometric model. As GEANT4-DNA is developing, the quasi-direct effects are yet to be fully explored in GEANT4-DNA.

TOPAS-nBio allows the building of plasmids of different lengths and shapes, nucleosomes, chromatin fibers, as well as a full human nucleus in the G0/G1 cycle stage, following the fractal 3D Hilbert curve [162]. Damage is reported following the Standard DNA Damage (SDD) specification defined by Schuemann et al. [163], which allows post-processing in the way desired by the user. Other outputs are also possible, such as a tally of the SSB and DSB, as well as their complexity, defined as the number of nucleotide moieties affected in a given damage site [164]. The mechanistic repair kinetics model DAMARIS for NHEJ, developed by Warmenhoven et al. [165], is also included as an extra stage in the GEANT4 simulation, taking the SDD file outputted by the physicochemical simulation. Recent focuses have been on developing a phenotype-specific nucleus model instead of using the Hilbert 3D curve to fill the space in a fractal pattern. A 'translator' of Hi-C data has been developed. This is a topological analysis of the connections across chromosomes [107]. TOPAS-nBio can generate a nucleus with spheres representing TADs as depicted in Hi-C assays. Each TAD is, in turn, composed of cubic voxels of different sizes (12, 24, and 48 nm side), which have arrangements of nucleosomes oriented in multiple ways. Additionally, 'linker' DNA strands are added wherever the voxels cannot naturally connect the double strands of DNA and between TADs so that the entire genetic material contained in the nucleus is connected. However, alongside geometrical advancements, GEANT4 tracking and scoring, at the chemical stage, is still a challenge due to the large size of these geometries. The subsequent release of TOPAS-nBio aims to provide fully functional simulations of DNA damage using this geometry. This would provide a sustainable method to create many cell-specific geometrical models for DNA damage analysis.

6. Conclusion and outlook

GEANT4-DNA can model geometries and provide biological analysis to the DNA level. GEANT4-DNA keeps developing towards closing the gap between physics, biology, and chemistry in Monte Carlo modelling for the analysis of biological damage from ionising radiation. This review has provided an overview of biological analysis and biological geometries that have been developed so far, highlighting the latest developments and future possible development avenues for GEANT4-DNA. The code has shown to be comparable to radiobiological studies in addition to evaluating energy distributions and biological damage to the DNA level which can be difficult to experimentally obtain in radiobiological studies. However, the biological analysis in simulation is also limited, due to the need of geometrical and cell-specific modelling in addition to the choice of algorithmic parameters used in the analysis models. Advances have been discussed in the review regarding the DNA, cellular, biological structures, cell population level modelling and use of cooperative platforms.

From this review, it can be summarised for accurate DNA quantification analysis of biological damage on a specific cell line, a cell model in GEANT4-DNA should contain the correct chemical composition of a cell, include sub-cellular components of the cell in addition to the DNA, cell-specific geometrical shape, DNA density and have the supporting physics and chemistry to account for indirect effects of the recently developed models which can be used and possibly to be included in GEANT4-DNA. Once cell-specific models are developed to contain realistic and accurate biological descriptions while maintaining computational efficiency, detailed

models about cell populations should be investigated further to enable the mimicry of a tissue-scale environment and biologically relevant damage of such radiobiological models. The environment would also include modelling simulations in cell media rather than arbitrary water and inclusion of cell-to-cell interactions and their effect on biological damage from irradiation. A way to include such a vast amount of biology, including the fourth dimension of time, could be to link GEANT4-DNA with biologically focused external platforms, such as CC3D.

Despite significant advancements in population geometric modelling, these platforms still face challenges in their analysis of physics and chemistry. In GEANT4-DNA, many models oversimplify the molecular composition of cells by assuming that they consist solely of water, neglecting the more complex chemical makeup of cytoplasm. However, some collaborative platforms, such as CompuCell3D, have made strides by incorporating advanced biological effects, such as the impact of time post-irradiation on cells and the influence of the ECM on cell populations, which can significantly affect the biological damage response following irradiation. Further exploration of the compatibility of these platforms with GEANT4 presents a promising opportunity to enhance geometric modelling in GEANT4-DNA. These advancements not only could improve the biological fidelity of models for radiobiological studies but also could extend analysis beyond DNA and DNA damage repair, including critical factors like the effects of the ECM. This holistic approach could lead to more accurate simulations and better understanding of cellular responses to radiation.

The topical software GEANT4-DNA is relatively new and hence can be geometrically expanded in different ways. It has been made evident that many of the advancements in the biological analysis and biological geometries have not been exploited to their full potential. However, the development of GEANT4-DNA, using the advances discussed in this review, provides a promising future of GEANT4-DNA to evaluate biological damage comparable to radiobiological studies.

Declaration of competing interest

The authors declare that they have no known competing financial interests or personal relationships that could have appeared to influence the work reported in this paper.

References

[1] J. Crowther, Some considerations relative to the action of X-rays on tissue cells, Proc. R. Soc. London Ser. B 96 (1924) 207–211.
[2] M. Curie, Sur l'étude des courbes de probabilité relatives à l'action des rayons X sur les bacilles, Comptes rendus l'Académie des Sci 188 (1929) 202–204.
[3] K.P. Chatzipapas, et al., Ionizing radiation and complex DNA damage: quantifying the radiobiological damage using Monte Carlo simulations, Cancers 12 (2020) 799.
[4] J.F. Fowler, 21 years of biologically effective dose, Br. J. Radiol. 83 (2010) 554–568.
[5] S.J. McMahon, K.M. Prise, Mechanistic modelling of radiation responses, Cancers 11 (2019) 205.
[6] S. Incerti, P. Barberet, B. Courtois, C. Michelet-Habchi, P. Moretto, Simulation of ion propagation in the microbeam line of CENBG using GEANT4, Nucl. Instrum. Methods Phys. Res. B 210 (2003) 92–97.
[7] I. Kyriakou, S. Incerti, H.N. Tran, C. Villagrasa, Y. Perrot. Geant4-DNA modelling of radiation effects in biological systems, Monte Carlo Techniques in Radiation Therapy, CRC press, 209–220, 2021.
[8] S. Agostinelli, et al., GEANT4—A simulation toolkit, Nucl. Instrum. Methods Phys. Res. a 506 (2003) 250–303.
[9] H. Nikjoo, D.T. Goodhead, Track structure analysis illustrating the prominent role of low-energy electrons in radiobiological effects of low-LET radiations, Phys. Med. Biol. 36 (1991) 229.
[10] S. Incerti, et al., Comparison of GEANT4 very low energy cross section models with experimental data in water, Med. Phys. 37 (2010) 4692–4708.
[11] L. Pandola, C. Andenna, B. Caccia, Validation of the Geant4 simulation of bremsstrahlung from thick targets below 3 MeV, Nucl. Instrum. Methods Phys. Res. B 350 (2015) 41–48.
[12] H. Nikjoo, D. Emfietzoglou, R. Watanabe, S Uehara, Can Monte Carlo track structure codes reveal reaction mechanism in DNA damage and improve radiation therapy? Radiat. Phys. 77 (2008) 1270–1279.
[13] S. Incerti, et al., The geant4-dna project, Int. J. Model. Simulat. Sci. Comput. 1 (2010) 157–178.
[14] W. Friedland, M. Dingfelder, P. Kundrát, P. Jacob, Track structures, DNA targets and radiation effects in the biophysical Monte Carlo simulation code PARTRAC, Mutation Res. 711 (2011) 28–40.
[15] D. Boscolo, M. Krämer, M. Durante, M.C. Fuss, E. Scifoni, TRAX-CHEM: a pre-chemical and chemical stage extension of the particle track structure code TRAX in water targets, Chem. Phys. Lett. 698 (2018) 11–18.
[16] F. Salvat, J.M. Fernández-Varea, J. Sempau, PENELOPE-2006: a code system for Monte Carlo simulation of electron and photon transport, in: Workshop Proceedings, 4, Citeseer, 2006, p. 7.
[17] GEANT4-DNA, Available on http://geant4-dna.in2p3.fr/styled-5/index.html.
[18] R. Brun, F. Rademakers, ROOT—An object oriented data analysis framework, Nucl. Instrum. Methods Phys. Res. a 389 (1997) 81–86.
[19] M.A. Bernal, et al., Track structure modeling in liquid water: a review of the Geant4-DNA very low energy extension of the Geant4 Monte Carlo simulation toolkit, Physica Medica 31 (2015) 861–874.
[20] S. Incerti, M. Douglass, S. Penfold, S. Guatelli, E. Bezak, Review of Geant4-DNA applications for micro and nanoscale simulations, Physica Medica 32 (2016) 1187–1200.
[21] I. Kyriakou, et al., Review of the geant4-dna simulation toolkit for radiobiological applications at the cellular and DNA level, Cancers 14 (2021) 35.
[22] K.P. Chatzipapas, et al., Simulation of DNA damage using Geant4-DNA: an overview of the" molecularDNA" example application, arXiv preprint (2022).
[23] F. Chappuis, et al., The general-purpose Geant4 Monte Carlo toolkit and its Geant4-DNA extension to investigate mechanisms underlying the FLASH effect in radiotherapy: current status and challenges, Physica Medica 110 (2023) 102601.
[24] I. Kyriakou, et al., Review of the Geant4-DNA simulation toolkit for radiobiological applications at the cellular and DNA level, Cancers 14 (2021) 35.
[25] I.R. Radford, G.S. Hodgson, J.P. Matthews, Critical DNA target size model of ionizing radiation-induced mammalian cell death, Int. J. Radiat. Biol. 54 (1988) 63–79.
[26] H. Tamaru, Confining euchromatin/heterochromatin territory: jumonji crosses the line, Genes Dev. 24 (2010) 1465–1478.
[27] M. Šefl, S. Incerti, G. Papamichael, D. Emfietzoglou, Calculation of cellular S-values using Geant4-DNA: the effect of cell geometry, Applied Radiation and Isotopes 104 (2015) 113–123.
[28] E. Charney, Genes, behavior, and behavior genetics, Wiley. Interdiscip. Rev. Cogn. Sci. 8 (2017) e1405.
[29] J.H.-C. Wang, B.P. Thampatty, J.-S. Lin, H.-J. Im, Mechanoregulation of gene expression in fibroblasts, Gene 391 (2007) 1–15.
[30] A. Ferraro, Altered primary chromatin structures and their implications in cancer development, Cellular Oncology 39 (2016) 195–210.
[31] A.C. Begg, F.A. Stewart, C. Vens, Strategies to improve radiotherapy with targeted drugs, Nat. Rev. Cancer 11 (2011) 239–253.

[32] S. Watanabe, et al., Morphologic studies of the liver cell dysplasia, Cancer 51 (1983) 2197–2205.
[33] W.-G. Shin, et al., Geant4-DNA simulation of the pre-chemical stage of water radiolysis and its impact on initial radiochemical yields, Physica Medica 88 (2021) 86–90.
[34] D. Jenkins. Radiation detection for nuclear physics, Interaction of ionising radiation with matter 2-1–2-23, IOP publishing, 2020.
[35] S. Incerti, et al., Geant4-DNA example applications for track structure simulations in liquid water: a report from the Geant4-DNA Project, Med. Phys. 45 (2018) e722–e739.
[36] M.U. Bug, et al., An electron-impact cross section data set (10 eV–1 keV) of DNA constituents based on consistent experimental data: a requisite for Monte Carlo simulations, Radiation Physics (College Park Md) and Chemistry (Easton) 130 (2017) 459–479.
[37] H.N. Tran, F. Chappuis, S. Incerti, F. Bochud, L. Desorgher, Geant4-DNA modeling of water radiolysis beyond the microsecond: an on-lattice stochastic approach, Int. J. Mol. Sci. 22 (2021) 6023.
[38] M. Karamitros, et al., Modeling radiation chemistry in the Geant4 toolkit, Prog. Nucl. Sci. Technol 2 (2011) 503–508.
[39] J. Ramos-Méndez, et al., Independent reaction times method in Geant4-DNA: implementation and performance, Med. Phys. 47 (2020) 5919–5930.
[40] I. Plante, L. Devroye, Considerations for the independent reaction times and step-by-step methods for radiation chemistry simulations, Radiation Physics (College Park Md) and Chemistry (Easton) 139 (2017) 157–172.
[41] S. Clement, et al., Mechanisms for tuning engineered nanomaterials to enhance radiation therapy of cancer, Advanced Science 7 (2020) 2003584.
[42] R. Weissleder, J. Wittenberg, M.G. Harisinghani, J.W. Chen, Primer of diagnostic imaging, August 17 (2011) 220–221.
[43] M.E. Lomax, L.K. Folkes, P. O'neill, Biological consequences of radiation-induced DNA damage: relevance to radiotherapy, Clin. Oncol. 25 (2013) 578–585.
[44] M. Mokari, M.H. Alamatsaz, H. Moeini, R. Taleei, A simulation approach for determining the spectrum of DNA damage induced by protons, Phys. Med. Biol. 63 (2018) 175003.
[45] N. Lampe, et al., Mechanistic DNA damage simulations in Geant4-DNA part 2: electron and proton damage in a bacterial cell, Physica Medica 48 (2018) 146–155.
[46] S. Meylan, et al., Simulation of early DNA damage after the irradiation of a fibroblast cell nucleus using Geant4-DNA, Sci. Rep. 7 (2017) 1–15.
[47] H. Nikjoo, P. O'Neill, W.E. Wilson, D.T. Goodhead, Computational approach for determining the spectrum of DNA damage induced by ionizing radiation, Radiat. Res. 156 (2001) 577–583.
[48] W. Friedland, et al., Comprehensive track-structure based evaluation of DNA damage by light ions from radiotherapy-relevant energies down to stopping, Sci. Rep. 7 (2017) 45161.
[49] W. Friedland, P. Jacob, P. Bernhardt, H.G. Paretzke, M. Dingfelder, Simulation of DNA damage after proton irradiation, Radiat. Res. 159 (2003) 401–410.
[50] D. Sakata, et al., Evaluation of early radiation DNA damage in a fractal cell nucleus model using Geant4-DNA, Physica Medica 62 (2019) 152–157.
[51] D. Müssig, *Re*-scanning in scanned ion beam therapy in the presence of organ motion. Doctoral Dissertation, Technische Universitat Darmstadt, 2014.
[52] F. Tommasino, et al., A DNA double-strand break kinetic rejoining model based on the local effect model, Radiat. Res. 180 (2013) 524–538.
[53] R.D. Stewart, Two-lesion kinetic model of double-strand break rejoining and cell killing, Radiat. Res. 156 (2001) 365–378.
[54] O.V. Belov, E.A. Krasavin, M.S. Lyashko, M. Batmunkh, N.H. Sweilam, A quantitative model of the major pathways for radiation-induced DNA double-strand break repair, J. Theor. Biol. 366 (2015) 115–130.
[55] M. Dos Santos, C. Villagrasa, I. Clairand, S Incerti, Influence of the DNA density on the number of clustered damages created by protons of different energies, Nucl. Instrum. Methods Phys. Res. B 298 (2013) 47–54.
[56] M. Ester, H.-P. Kriegel, J. Sander, X. Xu, A density-based algorithm for discovering clusters in large spatial databases with noise, KDD. 96 (1996) 226–231.
[57] J.A. Hartigan, M.A. Wong, Algorithm AS 136: a k-means clustering algorithm, J. R. Stat. Soc. Ser. C Appl. Stat. 28 (1979) 100–108.
[58] R.T. Ng, J. Han, Effcient and effective clustering methods for spatial data mining, in: Proceedings of VLDB, 1994, pp. 144–155.
[59] I.M. Khater, I.R. Nabi, G. Hamarneh, A review of super-resolution single-molecule localization microscopy cluster analysis and quantification methods, Patterns 1 (2020).
[60] E. Delage, et al., PDB4DNA: implementation of DNA geometry from the Protein Data Bank (PDB) description for Geant4-DNA Monte-Carlo simulations, Comput. Phys. Commun. 192 (2015) 282–288.
[61] H. Nikjoo, D.T. Goodhead, D.E. Charlton, H.G Paretzke, Energy deposition in small cylindrical targets by ultrasoft X-rays, Phys. Med. Biol. 34 (1989) 691.
[62] D. Sakata, et al., Prediction of DNA rejoining kinetics and cell survival after proton irradiation for V79 cells using Geant4-DNA, Physica Medica 105 (2023) 102508.
[63] H. Nikjoo, P. O'Neill, D.T. Goodhead, M. Terrissol, Computational modelling of low-energy electron-induced DNA damage by early physical and chemical events, Int. J. Radiat. Biol. 71 (1997) 467–483.
[64] D. Sakata, et al., Fully integrated Monte Carlo simulation for evaluating radiation induced DNA damage and subsequent repair using Geant4-DNA, Sci. Rep. 10 (2020) 1–13.
[65] R. Nakad, B. Schumacher, DNA damage response and immune defense: links and mechanisms, Front. Genet. 7 (2016) 147.
[66] B.M. Sirbu, D. Cortez, DNA damage response: three levels of DNA repair regulation, Cold. Spring. Harb. Perspect. Biol. 5 (2013) a012724.
[67] E. Mladenov, S. Magin, A. Soni, G. Iliakis, DNA double-strand-break repair in higher eukaryotes and its role in genomic instability and cancer: cell cycle and proliferation-dependent regulation, in: Seminars in Cancer Biology, 37, Elsevier, 2016, pp. 51–64.
[68] M. Suzuki, Y. Kase, H. Yamaguchi, T. Kanai, K. Ando, Relative biological effectiveness for cell-killing effect on various human cell lines irradiated with heavy-ion medical accelerator in Chiba (HIMAC) carbon-ion beams, Int. J. Radiat. Oncol. Biol. Phys. 48 (2000) 241–250.
[69] J.T. Finch, A. Klug, Solenoidal model for superstructure in chromatin, in: Proceedings of the National Academy of Sciences 73, 1976, pp. 1897–1901.
[70] C.L. Woodcock, L.-L. Frado, J.B. Rattner, The higher-order structure of chromatin: evidence for a helical ribbon arrangement, J. Cell Biol. 99 (1984) 42–52.
[71] D.E. Charlton, H. Nikjoo, J.L. Humm, Calculation of initial yields of single-and double-strand breaks in cell nuclei from electrons, protons and alpha particles, Int. J. Radiat. Biol. 56 (1989) 1–19.
[72] V. Michalik, M. Bĕgusova, Target model of nucleosome particle for track structure calculations and DNA damage modelling, Int. J. Radiat. Biol. 66 (1994) 267–277.
[73] M.A. Bernal, J.A. Liendo, An investigation on the capabilities of the PENELOPE MC code in nanodosimetry, Med. Phys. 36 (2009) 620–625.
[74] A. Peudon, S. Edel, M. Terrissol, Molecular basic data calculation for radiation transport in chromatin, Radiat. Prot. Dosimetry. 122 (2006) 128–135.
[75] P.D. Bank, Protein data bank, Nature New Biol. 233 (1971) 10–1038.
[76] K. Luger, A.W. Mäder, R.K. Richmond, D.F. Sargent, T.J. Richmond, Crystal structure of the nucleosome core particle at 2.8 Å resolution, Nature 389 (1997) 251–260.
[77] H. Nikjoo, P. Girard, A model of the cell nucleus for DNA damage calculations, Int. J. Radiat. Biol. 88 (2012) 87–97.
[78] S. Incerti, et al., Energy deposition in small-scale targets of liquid water using the very low energy electromagnetic physics processes of the Geant4 toolkit, Nucl. Instrum. Methods Phys. Res. B 306 (2013) 158–164.
[79] M. Dos Santos, C. Villagrasa, I. Clairand, S Incerti, Influence of the chromatin density on the number of direct clustered damages calculated for proton and alpha irradiations using a Monte Carlo code, Prog. Nucl. Sci. Technol. 4 (2014) 449–453.
[80] M. Bueno, R. Schulte, S. Meylan, C. Villagrasa, PO-0824: influence of the biological target volume modeling on ionization cluster-size distributions using Geant4-DNA, Radiother. Oncol. 115 (2015) S415–S416.
[81] M. Bueno, R. Schulte, S. Meylan, C. Villagrasa, Influence of the geometrical detail in the description of DNA and the scoring method of ionization clustering on nanodosimetric parameters of track structure: a Monte Carlo study using Geant4-DNA, Phys. Med. Biol. 60 (2015) 8583.
[82] M. Dos Santos, et al., Influence of chromatin condensation on the number of direct DSB damages induced by ions studied using a Monte Carlo code, Radiat. Prot. Dosimetry. 161 (2014) 469–473.
[83] M.A. Bernal, et al., An atomistic geometrical model of the B-DNA configuration for DNA–radiation interaction simulations, Comput. Phys. Commun. 184 (2013) 2840–2847.

[84] M.A. Bernal, et al., Performance of a new atomistic geometrical model of the B-DNA configuration for DNA-radiation interaction simulations, in: Journal of Physics: Conference Series 490, IOP Publishing, 2014, p. 12150.

[85] G. Raisali, L. Mirzakhanian, S.F. Masoudi, F. Semsarha, Calculation of DNA strand breaks due to direct and indirect effects of Auger electrons from incorporated 123I and 125I radionuclides using the Geant4 computer code, Int. J. Radiat. Biol. 89 (2013) 57–64.

[86] F. Semsarha, B. Goliaei, G. Raisali, H. Khalafi, L. Mirzakhanian, An investigation on the radiation sensitivity of DNA conformations to 60Co gamma rays by using Geant4 toolkit, Nucl. Instrum. Methods Phys. Res. B 323 (2014) 75–81.

[87] M. Tajik, A.S.H. Rozatian, F. Semsarha, Calculation of direct effects of 60Co gamma rays on the different DNA structural levels: a simulation study using the Geant4-DNA toolkit, Nucl. Instrum. Methods Phys. Res. B 346 (2015) 53–60.

[88] M. Tajik, A.S.H. Rozatian, F. Semsarha, Simulation of ultrasoft X-rays induced DNA damage using the Geant4 Monte Carlo toolkit, Nucl. Instrum. Methods Phys. Res. B 342 (2015) 258–265.

[89] S. Meylan, U. Vimont, S. Incerti, I. Clairand, C. Villagrasa, Geant4-DNA simulations using complex DNA geometries generated by the DnaFabric tool, Comput. Phys. Commun. 204 (2016) 159–169.

[90] E. Choi, K.S. Chon, M.G. Yoon, Evaluating direct and indirect effects of low-energy electrons using Geant4-DNA, Radiat. Effects Def. Solids 175 (2020) 1042–1051.

[91] K.P. Chatzipapas, et al., Quantification of DNA double-strand breaks using Geant4-DNA, Med. Phys. 46 (2019) 405–413.

[92] A. Zabihi, et al., Computational approach to determine the relative biological effectiveness of fast neutrons using the Geant4-DNA toolkit and a DNA atomic model from the Protein Data Bank, Phys. Rev. e 99 (2019) 52404.

[93] K.L. Cann, G. Dellaire, Heterochromatin and the DNA damage response: the need to relax, Biochem. Cell Biol. 89 (2011) 45–60.

[94] P. Venkatesh, I.V. Panyutin, E. Remeeva, R.D. Neumann, I.G. Panyutin, Effect of chromatin structure on the extent and distribution of DNA double strand breaks produced by ionizing radiation; comparative study of hESC and differentiated cells lines, Int. J. Mol. Sci. 17 (2016) 58.

[95] M.C. Elia, M.O. Bradley, Influence of chromatin structure on the induction of DNA double strand breaks by ionizing radiation, Cancer Res. 52 (1992) 1580–1586.

[96] I. Radulescu, K. Elmroth, B. Stenerlöw, Chromatin organization contributes to non-randomly distributed double-strand breaks after exposure to high-LET radiation, Radiat. Res. 161 (2004) 1–8.

[97] K. Magnander, R. Hultborn, K. Claesson, K. Elmroth, Clustered DNA damage in irradiated human diploid fibroblasts: influence of chromatin organization, Radiat. Res. 173 (2010) 272–282.

[98] K. Storch, et al., Three-dimensional cell growth confers radioresistance by chromatin density modification, Cancer Res. 70 (2010) 3925–3934.

[99] N. Tang, et al., Influence of chromatin compaction on simulated early radiation-induced DNA damage using Geant4-DNA, Med. Phys. 46 (2019) 1501–1511.

[100] T. Cremer, C. Cremer, Chromosome territories, nuclear architecture and gene regulation in mammalian cells, Nat. Rev. Genet. 2 (2001) 292–301.

[101] G. Bajpai, D.A. Pavlov, D. Lorber, T. Volk, S. Safran, Mesoscale phase separation of chromatin in the nucleus, Biophys. J. 118 (2020) 549a.

[102] Y. Thibaut, et al., Nanodosimetric calculations of radiation-induced DNA damage in a new nucleus geometrical model based on the isochore theory, Int. J. Mol. Sci. 23 (2022) 3770.

[103] J. Paces, et al., Representing GC variation along eukaryotic chromosomes, Gene 333 (2004) 135–141.

[104] X. Zhao, R. Liu, T. Zhao, F.J. Reynoso, Quantification of gold nanoparticle photon radiosensitization from direct and indirect effects using a complete human genome single cell model based on Geant4, Med. Phys. 48 (2021) 8127–8139.

[105] W.J. Kent, et al., The human genome browser at UCSC, Genome Res. 12 (2002) 996–1006.

[106] B.H. Lee, C.-K.C. Wang, A cell-by-cell Monte Carlo simulation for assessing radiation-induced DNA double strand breaks, Physica Medica 62 (2019) 140–151.

[107] S.P. Ingram, et al., Hi-C implementation of genome structure for in silico models of radiation-induced DNA damage, PLoS. Comput. Biol. 16 (2020) e1008476.

[108] T. Nagano, et al., Single-cell hi-C reveals cell-to-cell variability in chromosome structure, Nature 502 (2013) 59–64.

[109] L.J. Edens, K.H. White, P. Jevtic, X. Li, D.L. Levy, Nuclear size regulation: from single cells to development and disease, Trends. Cell Biol. 23 (2013) 151–159.

[110] J.F. Gillooly, A. Hein, R. Damiani, Nuclear DNA content varies with cell size across human cell types, Cold. Spring. Harb. Perspect. Biol. 7 (2015) a019091.

[111] Schuemann, J. et al. Features of TOPAS-NBio-Release 1.0. (2021).

[112] X. Zhao, R. Liu, T. Zhao, F.J. Reynoso, Modeling double-strand breaks from direct and indirect action in a complete human genome single cell Geant4 model, Biomed. Phys. Eng. Express. 6 (2020) 65010.

[113] S. Incerti, et al., Monte Carlo dosimetry for targeted irradiation of individual cells using a microbeam facility, Radiat. Prot. Dosimetry. 133 (2009) 2–11.

[114] Mercury® Computer Systems, Inc. Available on www.tgs.com/.

[115] J.A. Maxwell, J.L. Campbell, W.J. Teesdale, The Guelph PIXE software package, Nucl. Instrum. Methods Phys. Res. B 43 (1989) 218–230.

[116] F.-X. Arnaud, et al., Complex cell geometry and sources distribution model for Monte Carlo single cell dosimetry with iodine 125 radioimmunotherapy, Nucl. Instrum. Methods Phys. Res. B 366 (2016) 227–233.

[117] W.-G. Shin, et al., A Geant4-DNA evaluation of radiation-induced DNA damage on a human fibroblast, Cancers 13 (2021) 4940.

[118] J. Choi, G. Kim, S.Bin Cho, H.-J Im, Radiosensitizing high-Z metal nanoparticles for enhanced radiotherapy of glioblastoma multiforme, J. Nanobiotechnology 18 (2020) 122.

[119] W.-G. Shin, et al., Evaluation of the influence of physical and chemical parameters on water radiolysis simulations under MeV electron irradiation using Geant4-DNA, J. Appl. Phys. 126 (2019) 114301.

[120] D. Sakata, et al., Performance evaluation for repair of HSGc-C5 carcinoma cell using Geant4-DNA, Cancers 13 (2021) 6046.

[121] K. Chatzipapas, et al., Geant4-DNA simulation of human cancer cells irradiation with helium ion beams, Physica Medica 112 (2023) 102613.

[122] A. Ristic-Fira, O. Keta, V. Petkovic, G. Dordevic, S. Petringa, P. Cirrone, G. Cuttone, N.H. Tran, K. Chatzipapas, S. Incerti, P. I, Experimental validation of helium ions as a function of linear energy transfer in radioresistant human malignant cells, Int. J. Radiat. Biol. (2023).

[123] Y. Wang, et al., Multiple mesh-type real Human cell models for dosimetric application coupled with Monte Carlo simulations, Radiat. Res. (2023).

[124] A. Taheri, M.U. Khandaker, F. Moradi, D.A. Bradley, A review of recent advances in the modeling of nanoparticle radiosensitization with the Geant4-DNA toolkit, Radiat. Phys. 111146 (2023).

[125] E.M. Witkin, Genetics of resistance to radiation in Escherichia coli, Genetics 32 (1947) 221.

[126] O.V. Belov, M. Batmunkh, S. Incerti, O. Lkhagva, Radiation damage to neuronal cells: simulating the energy deposition and water radiolysis in a small neural network, Physica Medica 32 (2016) 1510–1520.

[127] G.A. Ascoli, D.E. Donohue, M.NeuroMorpho Halavi, Org: a central resource for neuronal morphologies, J. Neurosci. 27 (2007) 9247–9251.

[128] L. Bayarchimeg, M. Batmunkh, O. Belov, O. Lkhagva, Simulation of radiation damage to neural cells with the Geant4-DNA toolkit, in: EPJ Web of Conferences 173, EDP Sciences, 2018, p. 5005.

[129] N.B. Larsen, M. Rasmussen, L.J. Rasmussen, Nuclear and mitochondrial DNA repair: similar pathways? Mitochondrion 5 (2005) 89–108.

[130] S.J. McMahon, A.L. McNamara, J. Schuemann, K.M. Prise, H. Paganetti, Mitochondria as a target for radiosensitisation by gold nanoparticles, in: Journal of Physics: Conference Series 777, IOP Publishing, 2017, p. 12008.

[131] S. Zein, Monte Carlo simulations of 250 keV photons effects on a 3D realistic mitochondria phantom and evaluation of radiation enhancement using gold nanoparticles. Doctoral dissetation, Université Clermont Auvergne, France, 2017.

[132] C. Poole, I. Cornelius, J. Trapp, C. Langton, A CADinterface for GEANT4, Australas. Phys. Eng. Sci. Med. 35 (3) (2012) 329–334.

[133] Bitpalne Oxford Instruments, Available on www.bitplane.com/imaris.

[134] M.B. Tavakoli, H. Moradi, H. Khanahmad, M. Hosseini, Circular mitochondrial DNA: a Geant4-DNA user application for evaluating radiation-induced damage in circular mitochondrial DNA, J. Med. Signals Sens. 7 (2017) 213.

[135] N. D-Kondo, et al., DNA damage modeled with Geant4-DNA: effects of plasmid DNA conformation and experimental conditions, Phys. Med. Biol. 66 (2021) 245017.

[136] Y. Maayah, H. Nusrat, G. Pang, M. Tambasco, Assessing the DNA damaging effectiveness of ionizing radiation using plasmid DNA, Int. J. Mol. Sci. 23 (2022) 12459.

[137] J. Huang, T. Schlick, A. Vologodskii, Dynamics of site juxtaposition in supercoiled DNA, in: Proceedings of the National Academy of Sciences 98, 2001, pp. 968–973.

[138] D.L. Ermak, J.A. McCammon, Brownian dynamics with hydrodynamic interactions, J. Chem. Phys. 69 (1978) 1352–1360.

[139] J.C. Forster, M.J.J. Douglass, W.M. Phillips, E. Bezak, Stochastic multicellular modeling of x-ray irradiation, DNA damage induction, DNA free-end misrejoining and cell death, Sci. Rep. 9 (2019) 18888.

[140] J.C. Forster, M.J.J. Douglass, W.M. Harriss-Phillips, E. Bezak, Development of an in silico stochastic 4D model of tumor growth with angiogenesis, Med. Phys. 44 (2017) 1563–1576.

[141] G. Tamborino, et al., Modeling early radiation DNA damage occurring during 177Lu-DOTATATE radionuclide therapy, J. Nucl. Med. 63 (2022) 761–769.

[142] R. Liu, T. Zhao, M.H. Swat, F.J. Reynoso, K.A. Higley, Development of computational model for cell dose and DNA damage quantification of multicellular system, Int. J. Radiat. Biol. 95 (2019) 1484–1497.

[143] R. Salim, P. Taherparvar, Dosimetry assessment of theranostic auger-emitting radionuclides in a micron-sized multicellular cluster model: a Monte Carlo study using Geant4-DNA simulations, Appl. Radiat. Isotopes 188 (2022) 110380.

[144] P.A.K. Oliver, R.M. Thomson, A Monte Carlo study of macroscopic and microscopic dose descriptors for kilovoltage cellular dosimetry, Phys. Med. Biol. 62 (2017) 1417.

[145] M. Bĕgusová, et al., Radiosensitivity of DNA in a specific protein-DNA complex: the lac repressor-lac operator complex, Int. J. Radiat. Biol. 77 (2001) 645–654.

[146] Belloni, J., Mostafavi, M., Douki, T. & Spotheim-Maurizot, M. Radiation chemistry from basics to applications in material and life sciences. (2008).

[147] V. Štěpán, M. Davídková, Understanding radiation damage on sub-cellular scale using RADAMOL simulation tool, Radiat. Phys. (College Park Md) Chem. (Easton) 128 (2016) 11–17.

[148] R. Liu, et al., Development of a coupled simulation toolkit for computational radiation biology based on Geant4 and CompuCell3D, Phys. Med. Biol. 66 (2021) 45026.

[149] M.H. Swat, et al., Multi-scale modeling of tissues using CompuCell3D, in: Methods in Cell Biology, 110, Elsevier, 2012, pp. 325–366.

[150] D.M. Beazley, Automated scientific software scripting with SWIG, Future Gener. Comput. (Long Beach Calif) Syst. 19 (2003) 599–609.

[151] D.M. Beazley, Automated scientific software scripting with SWIG, Future Gener. Comput. (Long Beach Calif) Syst. 19 (2003) 599–609.

[152] Liu, R., Swat, M.H., Glazier, J.A., Powathil, G.G. & Higley, K.A. Computational simulation on radiation-induced gastrulation failure of chick embryo. *Available at SSRN* (2022) 4140058.

[153] L. Maigne, et al., CPOP: an open source C++ cell POPulation modeler for radiation biology applications, Physica Medica 89 (2021) 41–50.

[154] The CGAL Project. CGAL User and Reference Manual. 4.10 edition. CGAL Editorial Board, 2017, available on https://doc.cgal.org/latest/Manual/how_to_cite_cgal.html.

[155] K.P. Chatzipapas, P. Papadimitroulas, G. Loudos, N. Papanikolaou, G.C. Kagadis, IDDRRA: a novel platform, based on Geant4-DNA to quantify DNA damage by ionizing radiation, Med. Phys. 48 (2021) 2624–2636.

[156] Y. Thibaut, et al., MINAS TIRITH: a new tool for simulating radiation-induced DNA damage at the cell population level, Phys. Med. Biol. 68 (2023) 34002.

[157] D. Sakata, et al., Performance evaluation for repair of HSGc-C5 carcinoma cell using Geant4-DNA, Cancers 13 (2021) 6046.

[158] J. Schuemann, et al., TOPAS-nBio: an extension to the TOPAS simulation toolkit for cellular and sub-cellular radiobiology, Radiat. Res. 191 (2019) 125–138.

[159] S.G. Swarts, D. Becker, M. Sevilla, K.T. Wheeler, Radiation-induced DNA damage as a function of hydration. II. Base damage from electron-loss centers, Radiat. Res. 145 (1996) 304–314.

[160] M.G. Debije, M.D. Strickler, W.A. Bernhard, On the efficiency of hole and electron transfer from the hydration layer to DNA: an EPR study of crystalline DNA X-irradiated at 4 K, Radiat. Res. 154 (2000) 163–170.

[161] A. Bertolet, et al., Impact of DNA geometry and scoring on Monte Carlo track-structure simulations of initial radiation-induced damage, Radiat. Res. 198 (2022) 207–220.

[162] H. Zhu, et al., Cellular response to proton irradiation: a simulation study with TOPAS-nBio, Radiat. Res. 194 (2020) 9–21.

[163] Schuemann, A.J. et al. A new standard DNA damage (SDD) data format A new standard DNA damage (SDD) data format. (2019).

[164] A. Bertolet, I. Chamseddine, H. Paganetti, J. Schuemann, The complexity of DNA damage by radiation follows a gamma distribution: insights from the microdosimetric Gamma Model, Front. Oncol. 13 (2023) 1196502.

[165] J.W. Warmenhoven, et al., Insights into the non-homologous end joining pathway and double strand break end mobility provided by mechanistic in silico modelling, DNa Repair. 85 (2020) 102743.